ARTICLE

# Integrated bioinformatic analysis identifies key regulators and candidate biomarkers of cardiac fibrosis following acute myocardial infarction

Al James A. Manua*[1,2], Javier Lozano-Gerona[1], Mariel Lizbeth Joy S. Agsaoay[1], Ranelle Janine L. Asi[1], Conrad Allan C. Chong[1], and Ahmad Reza F. Mazahery[1]

[1]Institute of Biology, College of Science, University of the Philippines, Diliman, Quezon City, 1101 Philippines
[2]National Research Council of the Philippines, Department of Science and Technology, Bicutan, Taguig City, 1631 Philippines

**ABSTRACT**

Cardiac fibrosis, a hallmark of numerous cardiovascular diseases, is strongly associated with adverse outcomes such as heart failure. However, current therapies remain ineffective in halting its progression, largely because the underlying mechanisms and pathways are poorly understood. Traditional laboratory validation of candidate biomarkers is often labor-intensive, costly, and time-consuming. Hence, computational approaches have emerged as powerful tools to accelerate the identification of candidate biomarkers. This study, therefore, aims to identify key regulators and candidate biomarkers associated with cardiac fibrosis following acute myocardial infarction (AMI). Using an integrated bioinformatic approach, we retrieved eligible microarray datasets from the Gene Expression Omnibus (GEO) repository, identify differentially expressed genes (DEGs), constructed protein–protein interaction (PPI) networks, identify hub genes, and predicts the transcription factor–gene regulatory relationships and microRNA–mRNA regulatory networks. As a result, we found only GSE775 and GSE4648 datasets that met our criteria. Across shared 24 h and 48 h time points, we identified 565 common DEGs. Functional enrichment analysis revealed that inflammatory response and IL-17 signaling pathway are the major contributors to cardiac fibrosis progression. Network-based analysis revealed six highly connected hub genes - *Il1b, Itgam, Ccl2, Mmp9, Il6,* and *Ptgs2* - as central regulators of the fibrotic response. These hub genes are shown to be modulated by a network of transcription factors (NF-KB1, PPARA, FOS, EGR-1, and CEBPB) and microRNAs (mmu-miR-223-3p, mmu-miR-196b-5p, mmu-miR-181a-5p, mmu-miR-122-5p, and mmu-let-7c-5p), suggesting a multi-layered regulation of cardiac fibrosis progression. Collectively, the findings identify potential key regulators and candidate biomarkers of cardiac fibrosis following AMI. This integrative approach provides insights for future mechanistic studies, cross-species validation efforts and therapeutic exploration in cardiac fibrosis post-AMI.

*Corresponding author
Email Address: **aamanua@up.edu.ph**
Date received: 06 October 2025
Dates revised: 26 November 2025
Date accepted: 02 January 2026
DOI: https://doi.org/10.54645/2026191IQX-34

## INTRODUCTION

Cardiac fibrosis is a chronic scarring condition in the cardiac muscle characterized by the excessive and continuous deposition of extracellular matrix (ECM) proteins, particularly collagen type I deposition, which leads to impaired cardiac tissue function (Murtha et al. 2017). Fibrotic scarring of the cardiac muscle most often occurs after myocardial infarction, but other conditions, such as hypertensive heart disease, diabetic hypertrophic cardiomyopathy, and idiopathic dilated cardiomyopathy, also promote cardiac fibrosis (Hinderer & Schenke-Layland 2019). Currently, no FDA-approved drugs exist for treating cardiac fibrosis. This is partly because noninvasive methods like echocardiography cannot accurately measure fibrotic burden, and cardiac tissue samples are typically only available through invasive endomyocardial biopsies or during cardiac surgery (Travers et al. 2022). Most conventional therapies do not directly target fibrosis but instead address underlying cardiac dysfunction mechanisms, which are ineffective at slowing the progression of cardiac fibrosis (Zhang et al. 2018). Due to this therapeutic limitations, studies in biomarker discovery

**KEYWORDS**

cardiac fibrosis, acute myocardial infarction, biomarkers, IL-17 signaling pathway, differentially expressed genes, bioinformatics

has increased as essential tools in the fight against cardiac fibrosis and its critical role in the prognosis of cardiovascular diseases (Ding et al. 2020).

Due to the labor-intensive, costly, and time-consuming nature of traditional laboratory validation of biomarkers that uses *in vitro* and *in vivo* models, various computational methods have been developed to significantly accelerate the identification of candidate biomarkers (Yang et al. 2022). The most significant advanced analytical methods developed include high-throughput sequencing, microarray technologies, and bioinformatics. These innovations have enabled the discovery of key genes, molecular pathways, biological processes, and cellular behaviors, as well as a deeper understanding of critical genetic variations in cardiac fibrosis (Reid et al. 2016; Schafer et al. 2017). Despite advances in transcriptomics and microarray bioinformatics, there are still very scarce studies identifying potent biomarkers linked to cardiac fibrosis following AMI. To our knowledge, this is the first in silico study focused on cardiac fibrosis using a publicly available microarray dataset from a mouse model of AMI. This study, therefore, aims to identify key regulators and candidate biomarkers associated with post-AMI cardiac fibrosis by analyzing the gene expression data of heart tissues from the AMI mouse model from the Gene Expression Omnibus (GEO) database.

## MATERIALS AND METHODS

### Obtaining microarray gene expression datasets of interest

The overall analysis is outlined and represented in Figure 1 (Supplementary material). We downloaded the eligible microarray datasets from the Gene Expression Omnibus (GEO) database (https://www.ncbi.nlm.nih.gov/geo/). We analyzed and compared the gene expression profiles of the left ventricle (LV) of mice undergoing a sham operation (control group) and the infarcted tissue (IF) of AMI animals (experimental group) derived from GSE775 (Tarnavski et al. 2004) and GSE4648 (Harpster et al. 2006). The samples from the selected datasets were hybridized based on Affymetrix Murine Genome U74A Version 2 Array [MG_U74Av2] on a platform GPL81 (Affymetrix, Santa Clara, CA, USA).

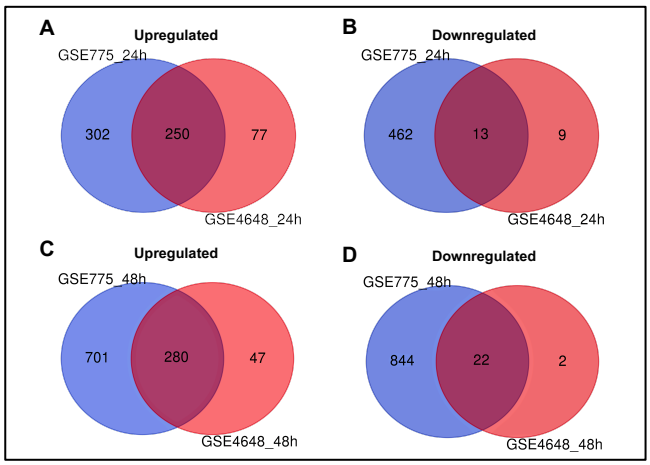


**Figure 1:** The overlapping upregulated and downregulated common DEGs between GSE775 and GSE4648 microarray datasets using Venn diagram. (A & B) 24h and (C & D) 48h.

### Identification of differentially expressed genes (DEGs)

By examining the raw expression data of GSE775 and GSE4648, differentially expressed genes (DEGs) between the AMI and sham-control groups were identified using the open web-based program, GEO2R. The shared time points - 1 h, 4 h, 24 h, and 48 h - between the two datasets were used for the subsequent analysis. Time points in only one dataset were disregarded to increase the study's accuracy. The entire gene expression dataset was normalized using the quantile normalization technique, and log2 transformed if necessary. It's considered statistically significant if a DEG's $|\log_2$ fold change$| > 1$ and its adjusted $P < 0.05$. In the following analysis, DEGs that were consistently upregulated and downregulated in both datasets were identified using the online Venn Diagram tool (http://bioinformatics.psb.ugent.be/webtools/Venn/). GraphPad Prism version 10.0.3 was used to create heat maps and volcano charts. When multiple probes mapped to the same gene, the expression of the gene was ascertained determined by taking the mean.

### Analysis of protein interaction networks and hub gene selection

Using the default settings of the Search Tool for Retrieval Interacting Genes (STRING) version 11.5 database (https://string-db.org/), we constructed the protein-protein interactions **(**PPI) network and the interacting proteins connected to DEGs (Szklarczyk et al. 2019). We restricted the species to "*Mus musculus*," and the confidence score was set at >0.4 (medium confidence score). The network's disconnected nodes were excluded. In the PPI network, a protein is represented as a node, and its interactions are represented as edges. The PPI network was displayed using Cytoscape v 3.10.1 (http://www.cytoscape.org/) (Shannon et al. 2003). Molecular Complex Detection (MCODE) plug-in of Cytoscape was used to extract top significant modules from the PPI network based on the following criteria: (i) "Degree cutoff = 2," (ii) "node score cutoff = 0.2," (iii) "k-core = 2," and (iv) "max depth = 100" (Bader & Hogue, 2003). The hub genes were identified using the built-in maximal clique centrality (MCC) algorithm of the Cytohubba plug-in for Cytoscape, which performed better (Chin et al. 2014). Using the online tool Draw Venn Diagram (http://bioinformatics.psb.ugent.be/webtools/Venn/), the overlapping hub genes between time points and major modules were discovered. Only hub genes were used for the subsequent analysis.

### Pathway Enrichment and Functional Annotation Analysis

Both the Gene Ontology (GO) analysis (Ashburner et al. 2000) and the KEGG pathway analysis (Ogata et al. 1999) were analyzed using the Metascape database (https://metascape.org/gp/index.html#/main/step1) (v3.5, San Diego, CA, USA) (Zhou et al. 2019). This analysis included the biological process, cellular component, and molecular function. The analysis was run under the default parameters: (i) A minimum count of three candidate proteins; (ii) An enrichment factor of >1.5. The information was collected and grouped according to how similar the members were. As the cutoff criterion, a significant level of $P < 0.05$ is established. To obtain the function and pathway terms for further visualization, GraphPad Prism version 10.0.3 was utilized.

### Predicting Transcription Factor-Hub Gene Interactions

We used TRRUST (Transcriptional Regulatory Relationships Unraveled by Sentence-based Text Mining) (Han et al. 2018), an online database, to predict the transcriptional regulatory networks capable of regulating the identified common hub genes. TRRUST produced an adjusted P-value, a significant level of $P < 0.05$ is established. Presented are only the TFs that were confirmed to be DEGs in both datasets at 24h and 48h.

### miRNA prediction for the hub genes

Using the miRNet program, we created the miRNA-mRNA regulatory network and predicted the miRNAs for the hub genes' important mRNAs, which we acquired from CytoHubba (Chang et al. 2020). The essential network, including all the seed genes, was also found by analyzing the created network using the Steiner Forest network (SFN) approach (Akhmedov et al. 2017).

**Statistical analysis**

For the statistical analysis, GraphPad Prism version 10.0.3 was utilized. The hub gene and transcription factor expression levels were validated using GSE775, and GSE4648. The statistical method employed to compare the expression levels between the AMI and sham-control groups was the independent sample t-test. If a P-value was < 0.05, it was deemed statistically significant.

## RESULTS AND DISCUSSION

**Gene expression analysis varies across datasets**

Differentially expressed genes (DEGs) related to cardiac fibrosis following AMI were identified at four common time points (1h, 4h, 24h, and 48h) using datasets GSE775 and GSE4648. A total of 3,364 DEGs were detected in GSE775 and 759 in GSE4648 (Supplementary Table 1A). Notably, the number of DEGs increased progressively with time, suggesting a dynamic transcriptional response as cardiac injury and remodeling advance. The temporal patterns of DEG distribution are illustrated by volcano plots in Figures 2 and 3 (Supplementary Material), highlighting the magnitude and direction of gene expression changes across both datasets.

Common DEGs between GSE775 and GSE4648 at each time point were identified using Venn diagram analysis, yielding a total of 571 shared genes (Supplementary Table 1B). No overlapping DEGs were detected at 1h, and only six upregulated DEGs emerged at 4h. In contrast, a marked increase was observed at later stages: 263 common DEGs at 24h (250 upregulated, 13 downregulated; Figures 1A–B) and 302 DEGs at 48h (280 upregulated, 22 downregulated; Figures 1C–D). A complete list of shared DEGs is provided in Supplementary Table 2. Given the limited overlap at the earlier time points (1h & 4h), subsequent analyses focused at 24h and 48h. Heatmap comparison further revealed dynamic shifts, with several DEGs upregulated at 24h but downregulated at 48h, and vice versa (Supplementary Figure 4). These findings highlight the temporal complexity of transcriptional regulation post-AMI, suggesting that key mediators, such as *Il6*, may play stage-specific roles in the progression of cardiac fibrosis.

**Functional enrichment analysis of differentially expressed genes**

To further elucidate the cellular roles of the common DEGs, GO analysis and KEGG pathway enrichment analyses were performed. At 24h, GO analysis indicated enrichment in processes related to the inflammatory response, external side of the plasma membrane, and cell adhesion molecule binding (Figure 2A). Corresponding KEGG analysis revealed significant involvement in the IL-17 signaling pathway, cytokine–cytokine receptor interaction, and hematopoietic cell lineage (Figure 2B). At 48h, GO terms were primarily enriched for inflammatory response, membrane raft, and actin binding (Figure 2C), while KEGG pathways included the IL-17 signaling pathway, Salmonella infection, and Phagosome (Figure 2D). Collectively, these findings suggest a time-dependent shift in biological function, with early transcriptional changes linked to signaling and adhesion processes, followed by the activation of immune- and inflammation-related pathways at later stages.

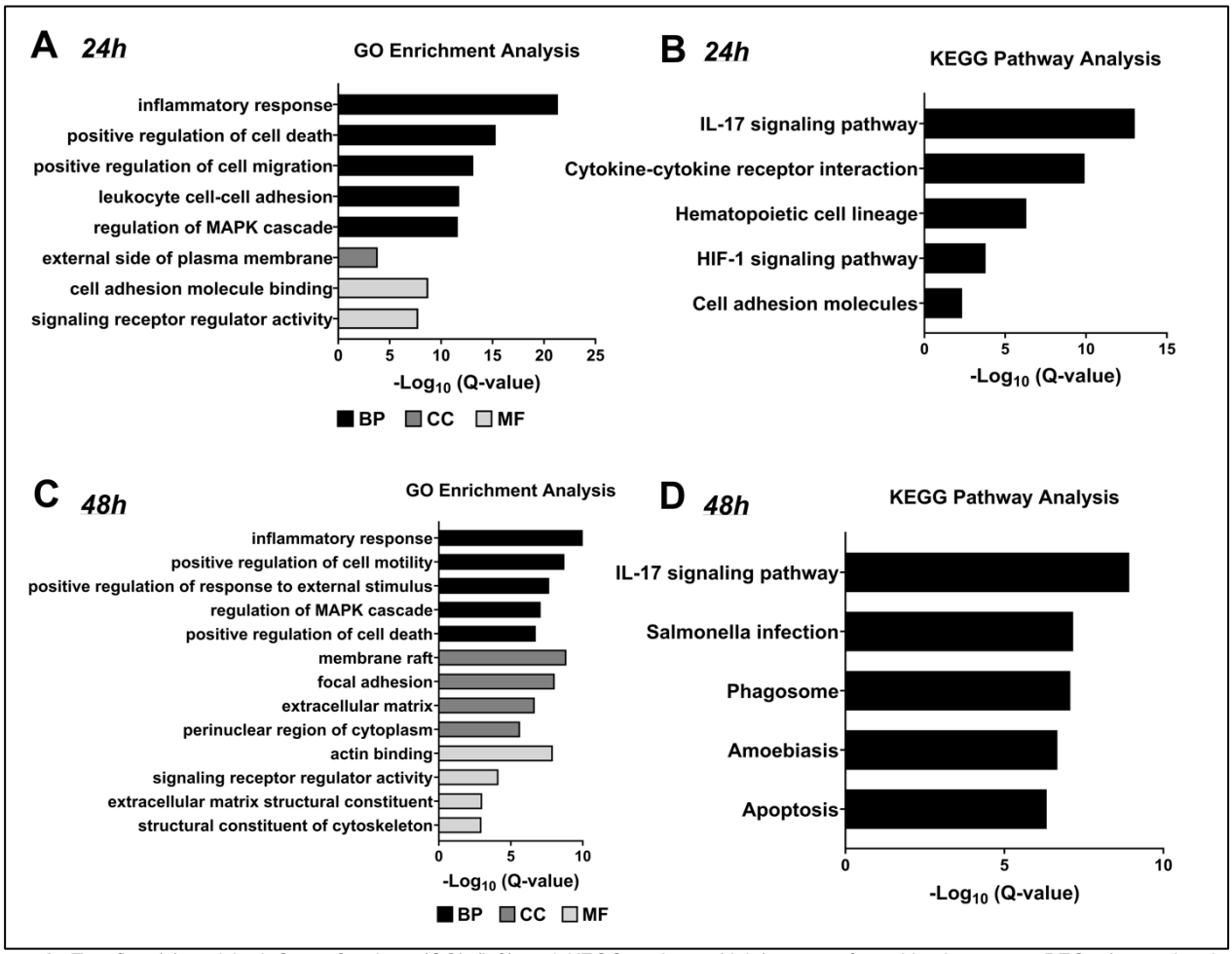


**Figure 2:** Top five (5) enriched Gene Ontology (GO) (left) and KEGG pathway (right) terms of combined common DEGs (upregulated and downregulated). (**A** & **B**) 24 h. (**C** & **D**) 48 h. GO: BP - Biological Process; CC - Cellular Components; MF - Molecular Functions. KEGG: Kyoto Encyclopedia of Genes and Genomes.

GO and KEGG pathway analyses revealed significant enrichment of DEGs in pathways related to the inflammatory response and the IL-17 signaling pathway. These results reinforce the growing consensus that inflammation is a defining feature of cardiac remodeling and fibrotic progression following myocardial infarction (MI) (Zhang et al. 2024). While the canonical TGF-β1/Smad signaling pathway has long been recognized as the principal driver of cardiac fibrosis (Saadat et al. 2021), our findings indicate that the IL-17 signaling pathway plays a significant role in this process. This observation is consistent with recent reports implicating IL-17–mediated signaling in myocardial remodeling and fibrosis after infarction (Chang et al. 2018; Sisto & Lisi 2024). In addition, tt was reported that IL-17 signaling pathway enhances the inflammatory response by increasing target mRNA transcription and promotes the functional activity of numerous target genes by controlling the stability of the transcribed mRNA via multiple pathways including NF-κB and MAPK pathways (Huangfu et al. 2023). Collectively, these findings not only expand the current understanding of fibrosis mechanisms but also position the IL-17 signaling pathway as a promising noncanonical therapeutic target for the prevention and treatment of post-MI cardiac fibrosis.

**Construction of network, analysis and extraction of modules**

To explore potential interactions among proteins encoded by the common DEGs, a protein–protein interaction (PPI) network was constructed using STRING and visualized in Cytoscape, with module extraction performed via the Cytoscape MCODE plugin. At 24h, the PPI network contained 256 nodes and 1,833 edges (Figure 3A), while at 48h, it expanded to 298 nodes and 1,918 edges (Figure 3B). Module analysis identified highly interconnected clusters at both time points: a 31-gene module with an MCODE score of 23.4 at 24h, and a 32-gene module with an MCODE score of 23.806 at 48h. These tightly connected modules may represent key regulators and potential biomarkers of AMI and cardiac fibrosis progression. The identification of such modules underscores the time-dependent reorganization of molecular interactions and provided the basis for hub gene selection in subsequent analyses.

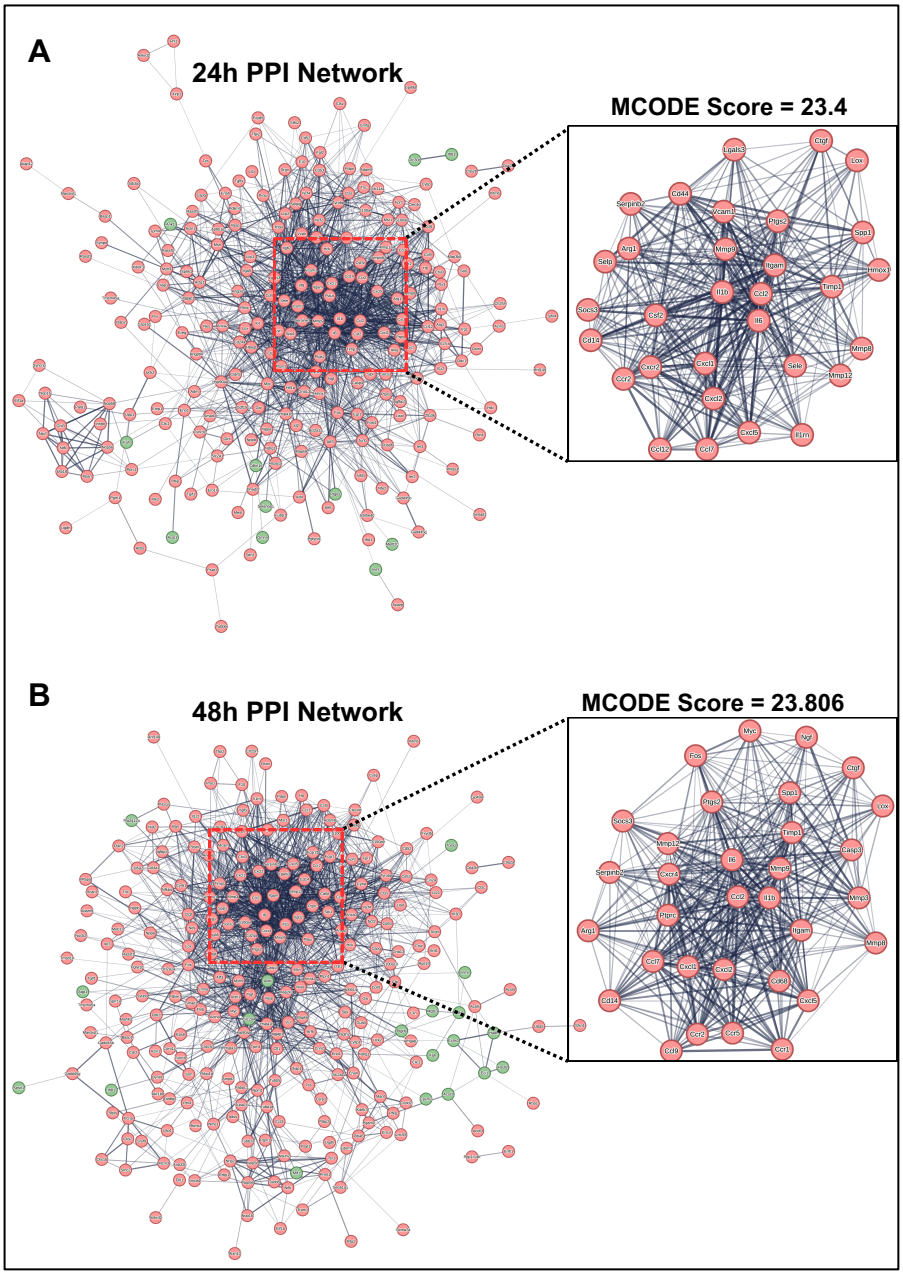


**Figure 3: Protein-Protein Interaction (PPI) network and module analysis.** Network analysis of common DEGs at (**A**) 24 h and (**B**) 48 h. Subsequently, MCODE plugin of Cytoscape revealed the Sub-network with the highest MCODE Score (right figures, inset). Upregulated DEGs are in red while downregulated DEGs are in green.

**Hub genes identification, functional enrichment and mRNA expression analysis**

Hub gene analysis was performed using the CytoHubba MCC algorithm in Cytoscape. The hub genes identified at 24h and 48h were intersected with the highly interconnected MCODE modules at each time point (Figures 5A–B, Supplementary Material). Venn diagram analysis (Figure 4A) revealed six overlapping hub genes: *Il1b, Itgam, Mmp9, Ccl2, Il6,* and *Ptgs2* (Figure 4B). These genes occupy central positions within the PPI network, suggesting they act as key regulators in the molecular landscape of post-AMI cardiac fibrosis. Notably, each has been independently implicated in inflammation, extracellular matrix remodeling, or fibrotic signaling, and prior studies have highlighted their roles in pathological cardiac remodeling. The convergence of these hub genes in our analysis underscores their potential as critical biomarkers and therapeutic targets for mitigating fibrotic progression following AMI.

Among the hub genes identified, *Il-6* and *Il1b* emerge as central proinflammatory mediators in post-AMI remodeling. Il-6 promotes collagen deposition and interstitial fibrosis, with genetic deletion or pharmacological inhibition shown to attenuate fibrosis and preserve cardiac function in preclinical models, hence, *Il6* could be a potential therapuetic target (Meléndez et al.,2010; González et al. 2015; Kumar et al. 2019; Gałdyszyńska et al. 2020). Similarly, *Il1b* contributes to cardiomyocyte apoptosis and fibrotic remodeling (Hwang et al. 2001; Blyszczuk et al. 2009), although it has been reported that *Il1b* exert anti-fibrotic effects under specific conditions (Brønnum et al. 2013). Integrin αM (Itgam/CD11b), a broadly expressed transmembrane receptor, promotes cardiomyocyte hypertrophy and fibroblast differentiation during hypertension-induced remodeling. Its selective inhibition mitigates adverse remodeling via multiple pathways (Israeli-Rosenberg et al. 2014; Zhang et al. 2024). Matrix metalloproteinase-9 (MMP-9), a key ECM-degrading enzyme, orchestrates inflammatory responses and contributes to fibrotic progression, while its inhibition confers protective effects against cardiac fibrosis (Deten et al. 2002; Iyer et al. 2016; Weng et al. 2016; Wang et al. 2024). Chemokine ligand 2 (CCL2/MCP-1) drives recruitment of CCR2+ monocytes and macrophages, facilitating fibroblast activation and matrix deposition, while disruption of its signaling reduces myofibroblast infiltration and attenuates fibrosis in ischemia–reperfusion models (Rollins 1996; Dewald et al. 2005; Dobaczewski & Frangogiannis 2009; Li & Frangogiannis 2021). Finally, Cyclooxygenase-2 (COX-2/Ptgs2), an inducible prostaglandin-synthesizing enzyme, is strongly upregulated post-MI; its inhibition, whether pharmacological or through natural compounds such as periplocymarin, has been shown to suppress fibrosis and improve myocardial metabolism (LaPointe et al. 2004; Rumzhum & Ammit 2016; Chi et al. 2017; Yun et al. 2021).

Gene Ontology analysis highlights the hub genes roles in regulating vascular endothelial growth factor production and cytokine activity, reflecting contributions to both inflammation and vascular remodeling (Figure 4C), whereas KEGG pathway analysis positions these genes within the IL-17 signaling axis (Figure 4D). Collectively, these six hub genes represent key molecular drivers of inflammation, extracellular matrix remodeling, and fibroblast activation in post-AMI pathology.

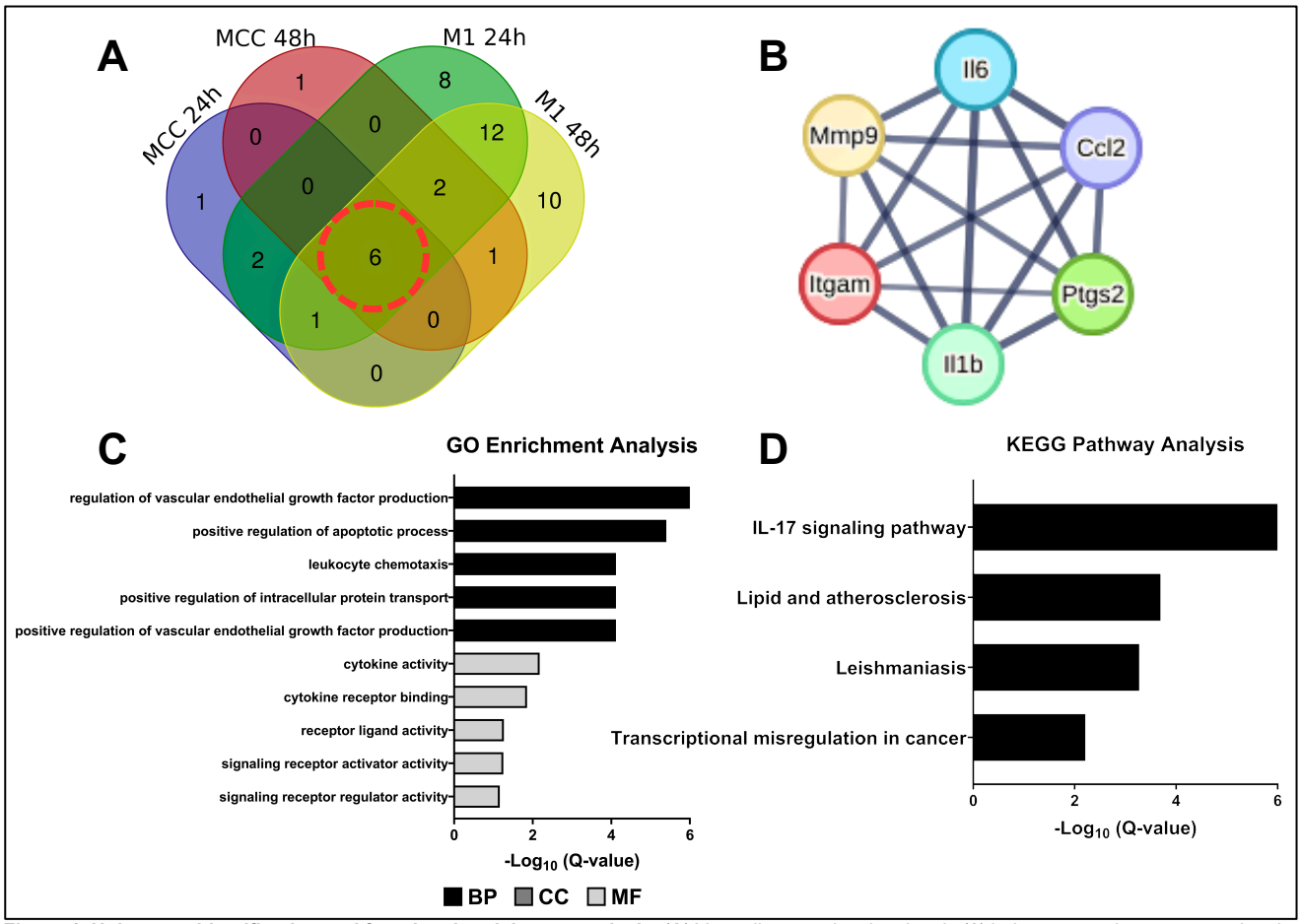


**Figure 4: Hub genes identification and functional enrichment analysis.** (**A**) Venn diagram showing the six (6) hub genes at the center overlapping between the MCC algorithm of Cytohubaa (at 24 h and 48 h) and Module 1 (M1, at 24 h and 48 h) of the PPI Network. (**B**) the six (6) hub genes. (**C**) Top five (5) highly enriched Gene Ontology terms using the six (6) hub genes. (**D**) Top five (5) highly enriched KEGG pathway of six (6) hub genes GO: BP - Biological Process; CC - Cellular Components; MF - Molecular Functions. KEGG: Kyoto Encyclopedia of Genes and Genomes.

Validation using the GSE775 and GSE4648 datasets confirmed differential expression of all six hub genes (*Il1b, Itgam, Mmp9, Ccl2, Il6,* and *Ptgs2)* in AMI samples. In GSE775, mRNA expression of all six hub genes was significantly upregulated in AMI versus control samples at 24h and 48h ($P < 0.01$, Figure 5A-B). In GSE4648, all six-hub gene were upregulated at 24h ($P < 0.05$, Figure 5C), while only *Il1b, Mmp9, Ccl2,* and *Ptgs2* were significantly upregulated at 48h ($P < 0.05$, Figure 5D). These results corroborate their active involvement in post-infarction inflammation and fibrosis, reinforcing their potential as therapeutic targets to mitigate cardiac remodeling and prevent progression to heart failure.

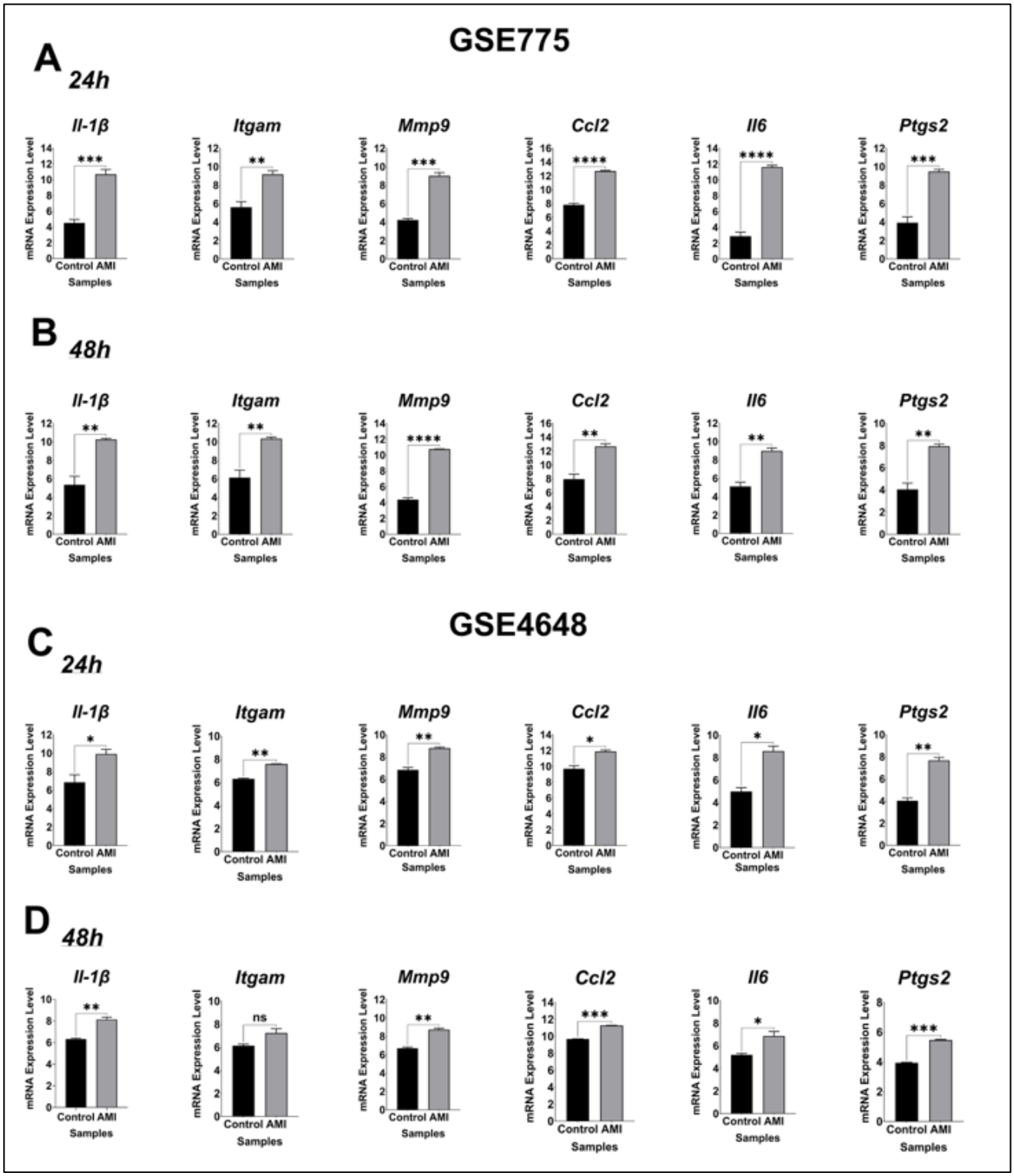


**Figure 5: mRNA expression levels of the six (6) common hub genes.** (**A**) 24 h and (**B**) 48 h in GSE775; (**C**) 24 h and (**D**) 48 h in GSE4648. Data is presented as mean ± SEM. A p-value < 0.05 was considered statistically significant relative to the control. *p-value < 0.05; **p-value < 0.01; ***p-value <0.001; ****p-value <0.0001; ns - not significant.

Notably, many of these hub genes—particularly *Il6*, *Il1b*, CCL2, and MMP9—are recognized downstream effectors and regulated by IL-17 signaling axis (Amatya et al. 2017). This mechanistic link underscores the relevance of the IL-17 pathway in coordinating the activity of these hub genes, may provide strategies for designing

novel therapeutic strategies for IL-17-mediated signaling and inflammation (Amatya et al. 2017).

**Mapping the Transcription factors-Hub gene interaction landscape**

Cardiac transcription factors (TFs) are critical regulators of cardiac remodeling, influencing fibrosis by modulating gene expression related to hypertrophy and fibroblast activation (Hong & Zhang 2022). To elucidate potential upstream regulators of the six hub genes (*Il1b, Itgam, Ccl2, Mmp9, Il6*, and *Ptgs2*), we performed TRRUST analysis and assessed their differential expression in the GSE775 and GSE4648 datasets. A total of 17 TFs were initially predicted (see Supplementary Table 2); however, only a five (5) TFs (i.e., NFKB1, PPARA, EGR1, FOS and C/EBPβ) exhibited differential expression across both datasets as shown in Table 1. These findings highlight a set of transcriptional regulators that may orchestrate hub-gene expression following AMI inflammatory and fibrotic responses, providing mechanistic insight into the regulatory networks driving cardiac fibrosis progression.

**Table 1: Key transcription factors (TFs) of hub genes.** Presented are the validated TFs to be differentially expressed in both datasets at 24h and 48h.

| Key TF | Description | Hub genes | *p-value* |
|---|---|---|---|
| NFKB1 | nuclear factor of kappa light polypeptide gene enhancer in B cells 1, p105 | *Il1b, Itgam, Ccl2, Mmp9, Il6, Ptgs2* | 8.36E-13 |
| C/EBPβ | CCAAT/enhancer binding protein (C/EBP), beta | *Il1b, Il6, Ptgs2* | 1.63E-07 |
| EGR1 | early growth response 1 | *Il1b, Ccl2, Mmp9* | 8.08E-07 |
| PPARA | peroxisome proliferator-activated receptor alpha | *Il6, Ptgs2* | 7.46E-05 |
| FOS | FBJ osteosarcoma oncogene | *Mmp9, Il6* | 0.000111 |

Nuclear factor-KB (NFKB), is a central mediator of inflammatory signaling and traditionally viewed as a proinflammatory driver of adverse remodeling (Kawamura et al. 2005; Brown et al. 2005; Frantz et al. 2006; Kawano et al. 2006; Tas et al. 2009). Emerging evidence suggests a context-dependent cardioprotective role for NFKB, including anti-inflammatory signaling, ECM remodeling, and oxidative stress mitigation (Santos et al. 2010). Peroxisome proliferator-activated receptor α (PPARα), is a key regulator of fatty acid oxidation and metabolic homeostasis, also modulates cardiac inflammation (Lin et al. 2022). PPARα deficiency reported to increase expression of fibrotic (collagen I, MMP-2) and inflammatory (IL-6, TNF-α, COX-2) markers (Smeets et al. 2008). PPARα activation by fenofibrate attenuates fibrosis and inflammation in *Trypanosoma cruzi*–infected mice by downregulating MMP-9 and connective tissue growth factor (CTGF) (Cevey et al. 2017). The FOS family of transcription factors (Fos, FosB, Fra-1, Fra-2), components of the AP-1 complex, are highly expressed in cardiac fibroblasts and contribute to hypertrophy, inflammation, and fibrosis (Dai et al. 2013; Wang et al. 2009; Whitehead et al. 2023). Among these, Fos-like 2 (Fra-2/Fosl2) has been specifically linked to exacerbated myocardial fibrosis, arrhythmogenesis, and maladaptive stress responses under immunofibrotic conditions (Seidenberg et al. 2021; Stellato et al. 2023). Early growth response-1 (Egr-1), a master transcriptional regulator of inflammatory and apoptotic genes and its silencing mitigates myocardial injury and remodeling (Khachigian 2006; Rayner et al. 2013). CCAAT/enhancer-binding protein β (C/EBPβ), a member of the C/EBP transcription factor family, has also been implicated in fibrotic signaling cascades in the heart and other organs (Wang et al. 2022a).

Further expression analysis revealed that NFKB1, EGR1, FOS (both in 24h and 48h) and C/EBPβ (48h only) were significantly upregulated in AMI samples, whereas PPARA was higher in controls both in GSE775 and GSE4648 ($P < 0.05$, Figure 6A-D); only FOS at 48h in GSE4648 was not significantly elevated ($P > 0.05$, Figure 6D). These results underscore the complex and dynamic regulatory roles of TFs, with distinct temporal and dataset-dependent patterns.

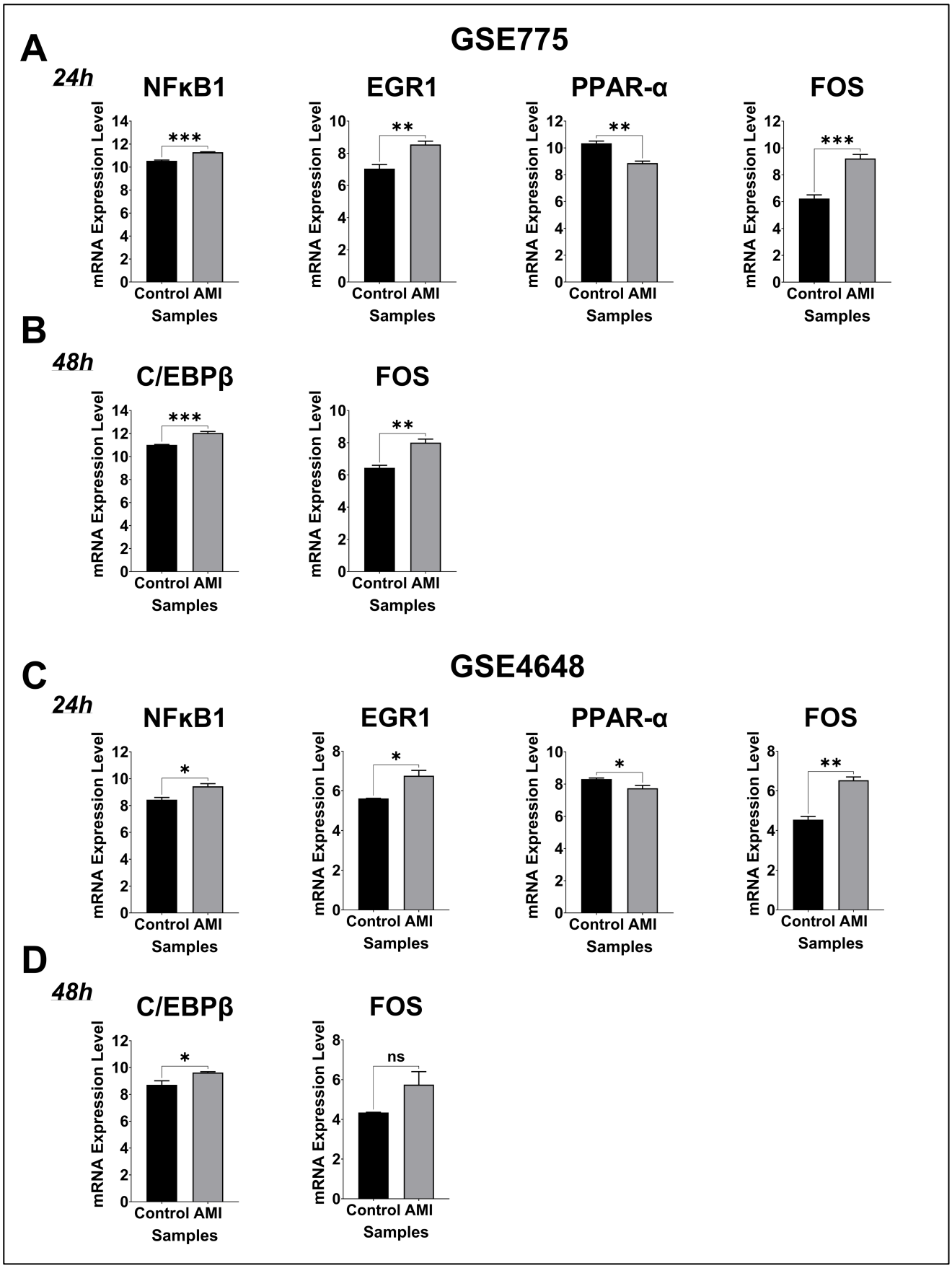


**Figure 6: mRNA expression levels of differentially expressed transcription factors (TFs).** (**A**) 24 h and (**B**) 48 h in GSE775; (**C**) 24 h and (**D**) 48 h in GSE4648. Data is presented as mean ± SEM. A p-value < 0.05 was considered statistically significant relative to the control. *p-value < 0.05; **p-value < 0.01; ***p-value <0.001; ns - not significant.

Interestingly, both NFKB and C/EBPβ pathways are reported to be regulated by the IL-17 signaling axis, which modulates the expression of downstream target genes and can either activate or inhibit these pathways via feedback regulation (Amatya et al. 2017; Huangfu et al. 2023). Despite these insights, further studies are needed to elucidate how NFKB and C/EBPβ can be precisely

manipulated *in vitro* to maintain immune homeostasis and develop targeted therapeutic strategies (Vidal et al. 2021).

**Mapping the miRNA-Hub gene interaction landscape**

MicroRNAs (miRNAs) are small, non-coding RNAs that modulate gene expression primarily by regulating mRNA translation and degradation (Balasundaram & Priya, 2023). They have been implicated as critical regulators of cardiac fibrosis through their targeting of extracellular matrix (ECM)–related genes and components of the TGF-β signaling pathway (Wang et al. 2016). Owing to their central role in fibrotic remodeling, miRNAs are increasingly recognized as promising therapeutic targets (Samanta et al. 2016).

To further elucidate the regulatory mechanisms influencing the identified hub genes, a miRNA-gene interaction network was constructed using the miRnet tool. This network aimed to identify key miRNAs involved in the regulation of top hub genes and explore potential post-transcriptional regulatory relationships. As a result, initially, there were 51 nodes (six genes and 45 miRNAs) and 68 edges in the miRNA–mRNA network (Figure 7A). The network was subsequently examined using the Steiner Forest network in miRnet and revealed 11 nodes (six genes and five miRNAs) and ten edges (Figure 7B). These findings suggest a more refined regulatory interaction between miRNAs and hub genes, with a reduced set of miRNAs playing a central role in modulating gene expression within the identified network. In the present study, we constructed a putative miRNA–mRNA regulatory network, revealing that the six hub genes—*Il-6, Il1b, Itgam, Mmp9, Ccl2* and *Ptgs2* - are likely regulated by mmu-miR-223-3p, mmu-miR-196b-5p, mmu-miR-181a-5p, mmu-miR-122-5p and mmu-let-7c-5p.

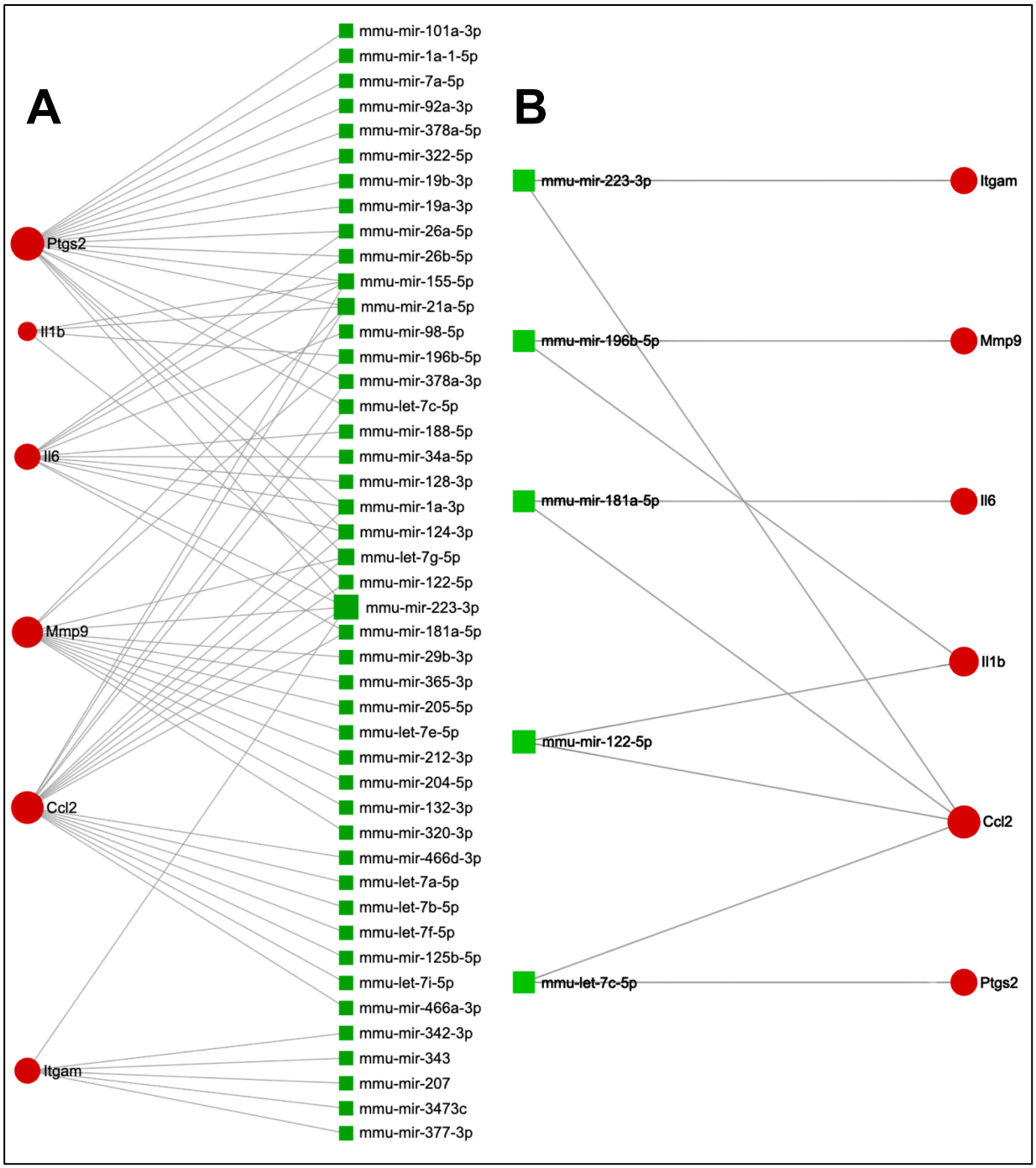


**Figure 7: The miRNA–mRNA regulatory network of six (6) common hub genes.** (**A**) The initial miRNA–mRNA network using miRnet; (**B**) The final miRNA–mRNA network using miRnet with the Steiner Forest network method. The green squares represent miRNAs, while the red circles represent mRNAs (6 common hub genes).

The miR-223-3p used to be called miR-223 and was reported to promote hypoxia-induced cardiomyocyte injury (Tang et al. 2018) and induce myocardial fibrosis (Liu et al. 2016). However, miR-223-3p was also reported to exert protective effects on the I/R-induced inflammatory response and cardiomyocyte necroptosis (Qin et al. 2016). An earlier study established that the downregulated endothelial miR-196b-5p inhibits the angiogenic functions of endothelial cells *in vitro* and suppressed skin wound healing *in vivo* (Ren et al. 2023). A recent study also reported that overexpression of miR-196b-5p regulates fibrosis *in vitro* by suppressing TGF-β-induced upregulation of COL1A2 (Baral et al. 2021) and reduce production of inflammatory cytokines, such as IL-6 and TNF-α (Yuan et al. 2018). The miR-181 family regulates vascular inflammation and immunity (Sun et al. 2014). It was reported that miR181a-5p overexpression was also found to inhibit myocardial inflammation and oxidative stress *in vitro* by targeting activating transcription factor 2 (ATF2) (Liu et al. 2020).

MiR-122-5p has pleiotropic biological functions, and its level is correlated with liver fibrosis (Cao et al. 2018). However, previous study demonstrated that by upregulating the expression of miR-122-5p, it inhibits isoproterenol-induced myocardial fibrosis *in vivo* (Wang et al. 2022b), however, it exacerbates angiotensin II-induced cardiac fibrosis and dysfunction in hypertensive rats (Song et al. 2022). As a member of the let-7 family, let-7c-5p is essential for cell growth and proliferation (Hertel et al. 2012). Let-7c-5p was upregulated in patients with advanced heart failure compared with healthy patients, which supports using these microRNAs as potential biomarkers and might be involved in disease progression, including cardiac fibrosis (Marques et al. 2016).

This study identifies a set of candidate biomarkers—including hub genes, transcription factors, and microRNAs—that may inform the development of targeted therapeutic strategies for acute myocardial infarction (AMI). Future studies should validate these findings through quantitative assessments of RNA and protein expression levels in both in vitro and, ideally, in vivo models. Based on our analysis, we anticipate a pronounced upregulation of the identified biomarkers within 24–48h following AMI. Notably, the inflammatory response and IL-17 signaling pathway emerged as key drivers of cardiac fibrosis, highlighting their potential as therapeutic targets. Existing treatments, such as plasmapheresis or therapeutic plasma exchange, may serve as adjunctive therapies for high-risk AMI patients. However, the success of such interventions hinges on the identification of precise biomarkers to guide treatment selection and timing. While animal models remain essential for mechanistic validation, their cost, complexity, and duration pose practical limitations. In this context, computational approaches offer a scalable, efficient alternative for early-stage biomarker discovery, providing a foundation for hypothesis-driven experimental studies.

This study has several limitations. First, the analysis was conducted entirely in silico and requires validation through experimental models. Second, due to limited availability of suitable datasets, only two relevant mouse microarray datasets modeling AMI were analyzed. Third, one of these datasets (GSE4648) includes only two biological replicates per group, which may limit statistical power and the resolution of differentially expressed gene (DEG) identification. Lastly, reliance on mouse data constrains direct translational relevance, underscoring the need for expanded datasets and cross-species validation in future studies.

## CONCLUSION

In conclusion, this study presents a comprehensive bioinformatics analysis of differentially expressed genes and signaling pathways implicated in cardiac fibrosis following AMI. The key findings of the study was the identification of key regulators and candidate biomarkers potentially involved in the progression of cardiac fibrosis following AMI. These key regulators and biomarkers, while previously associated with AMI, may also contribute to fibrotic remodeling, as supported by existing literature, and may be use in disease screening and detection, diagnosis and drug development. Our findings shows the multifaceted landscape of cardiac fibrosis following AMI and offer a foundation for the development of targeted therapies. Further mechanistics validation through in vitro and in vivo experiments is recommended to further support the findings translational clinical applications.

## ACKNOWLEDGMENTS

The authors extend their gratitude to the Commission on Higher Education - Philippine California Advanced Research Institutes (CHED-PCARI) (Grant no. IHITM 2018-033) for the grant provided that made this research possible.

## CONFLICT OF INTEREST

The authors declare that there is no conflict of interest.

## CONTRIBUTIONS OF INDIVIDUAL AUTHORS

AJAM, JLG, and CAC conceptualized and design of study. AJAM, MLJA, and CAC acquired all necessary raw data. AJAM, JLG, and ARM performed the analysis and/or interpretation of data, and prepared all the tables and figures. AJAM and JLG wrote the original draft. AJAM, JLG, MLJA, RJA, CAC, and ARM revised the manuscript for significant intellectual content. All authors reviewed the manuscript, contributed to the final manuscript and approved for publication.

## REFERENCES

Akhmedov M, Lenail, A, Bertoni F, Kwee I, et al. A Fast Prize-Collecting Steiner Forest Algorithm for Functional Analyses in Biological Networks. In: Salvagnin, D., Lombardi, M. (Eds) Integration of AI and or Techniques in Constraint Programming. Cpaior 2017. Lecture Notes in Computer Science. 2017;263–76.

Amatya N, Garg AV, & Gaffen SL. IL-17 Signaling: The Yin and the Yang. *Trends in immunology*. 2017;*38*(5), 310–322.

Ashburner M, Ball CA, Blake JA, et al. Gene Ontology: Tool for the Unification of Biology. Nature Genetics. 2000;25(1): 25–9.

Bader GD, & Hogue CW. An Automated Method for Finding Molecular Complexes in Large Protein Interaction Networks. BMC Bioinformatics. 2003;4;2.

Balasundaram A, Priya G. In Silico Analysis Revealed the Potential CircRNA-MiRNA-mRNA Regulative Network of Non-Small Cell Lung Cancer (NSCLC). Computers In Biology and Medicine. 2023;152: 106315–5.

Baral H, Uchiyama A, Yokoyama Y, et al. Antifibrotic Effects and Mechanisms of Mesenchymal Stem Cell-Derived Exosomes in a Systemic Sclerosis Mouse Model: Possible Contribution of Mir-196b-5p. Journal of Derm. Science. 2021;104(1): 39–47.

Blyszczuk P, Kania G, Dieterle T, Marty RR, et al. Myeloid Differentiation Factor-88/Interleukin-1 Signaling Controls

Cardiac Fibrosis and Heart Failure Progression in Inflammatory Dilated Cardiomyopathy. Circ Res. 2009;105(9): 912–920.

Brønnum H, Eskildsen T, et al. Il-1β Suppresses TGF-B-Mediated Myofibroblast Differentiation in Cardiac Fibroblasts. Growth Factors. 2013;31(3), 81–89.

Brown MT, et al. Cardiac-Specific Blockade of Nf-Kb in Cardiac Pathophysiology: Differences Between Acute and Chronic Stimuli *in vivo*. 2005;289(1): H466–76.

Cevey ÁC, Mirkin GA, Donato M, Rada MJ, et al. Treatment with Fenofibrate plus, a low dose of Benznidazole attenuates cardiac dysfunction in experimental Chagas disease. Int'l J. for Parasitology: Drugs and Drug Resistance. 2017;7(3), 378-387.

Chang L, Zhou G, et al. Mirnet 2.0: Network-Based Visual Analytics for MiRNA Functional Analysis and Systems Biology. Nucleic Acids Res. 2020; 48(W1): W244–51.

Chang SL, Hsiao YW, et al. Interleukin-17 Enhances Cardiac Ventricular Remodeling via Activating MAPK Pathway in Ischemic Heart Failure. 2018;122: 69–79.

Chi YC, Shi Cl, Zhou M, Liu Y, Zhang G, & Hou SA. Selective Cyclooxygenase-2 Inhibitor Ns-398 Attenuates Myocardial Fibrosis in Mice after Myocardial Infarction via Snail Signaling Pathway. Euro. Review for Med. and Phar. Sci. 2017;21(24): 5805–5812.

Chin CH, Chen SH, Wu HH, Ho CW, et al. Cytohubba: Identifying Hub Objects and Sub-Networks from Complex Interactome. BMC Systems Biology. 2014;8(Suppl 4): S11.

Dai Y, Khaidakov M, Wang X, Ding Z, Su W, et al. MicroRNAs involved in the regulation of postischemic cardiac fibrosis. Hypertension. 2013;61(4), 751–756.

Deten A, Volz HC, Briest W, Zimmer HG. Cardiac Cytokine Expression Is Upregulated in the Acute Phase after Myocardial Infarction. Experimental Studies in Rats. Cardiovasc Res. 2002;55: 329–340.

Dewald O, Zymek P, Winkelmann K, Koerting A, Ren G, et al. Ccl2/Monocyte Chemoattractant Protein-1 Regulates Inflammatory Responses Critical to Healing Myocardial Infarcts. Circulation Research. 2005;96(8): 881–9.

Ding Y, Wang Y, Zhang W, Jia Q, Wang X, Li Y, Lu S, & Zhang J. Roles of Biomarkers in Myocardial Fibrosis. Aging and Disease. 2020;11(5), 1157–1174.

Dobaczewski M & Frangogiannis NG. Chemokines and Cardiac Fibrosis. Frontiers In Bioscience. 2009;1(2): 391–405.

Frantz S, Hu K, Bayer B, et al. Absence of NF-κB Subunit P50 Improves Heart Failure after Myocardial Infarction. The Faseb Journal. 2006;20(11): 1918–20.

Gałdyszyńska M, Bobrowska J, Lekka M, et al. The Stiffness-Controlled Release of Interleukin-6 By Cardiac Fibroblasts is Dependent on Integrin A2β1. Journal Of Cellular and Molecular Medicine. 2020;24(23): 13853–13862.

González GE, Rhaleb NE, et al. Deletion of Interleukin-6 Prevents Cardiac Inflammation, Fibrosis, And Dysfunction Without Affecting Blood Pressure in Angiotensin Ii-High Salt-Induced Hypertension. J. of Hypertension. 2015;33(1): 144–52.

Han H, Cho JW, Lee S, Yun A, Kim H, Bae D, et al. TRRUST V2: An Expanded Reference Database of Human and Mouse Transcriptional Regulatory Interactions. Nucleic Acids Research. 2018;46(D1): D380–6.

Harpster MH, Bandyopadhyay S, et al. Earliest Changes in the Left Ventricular Transcriptome Post-Myocardial Infarction. Mamm. Genome. 2006;17(7): 701–15.

Hertel J, Bartschat S, Wintsche A, Otto C, Stadler PF. Evolution of the let-7 microRNA Family. RNA Biology. 2012;9(3): 231–41.

Hinderer S & Schenke-Layland K. Cardiac fibrosis – A short review of causes and therapeutic strategies. Advanced Drug Delivery Reviews. 2019;146.

Hong JH & Zhang HG. Transcription Factors involved in The Development and Prognosis of Cardiac Remodeling. Frontiers In Pharmacology. 2022;13, 828549.

Huangfu L, Li R, Huang Y. et al. The IL-17 family in diseases: from bench to bedside. Sig Transduct Target Ther. 2023;8, 402.

Hwang MW, Matsumori A, Furukawa Y, et al. Neutralization of Interleukin-1β in the Acute Phase of Myocardial Infarction Promotes the Progression of Left Ventricular Remodeling. J. of the American College of Cardiology. 2001;38(5): 1546–53.

Israeli-Rosenberg S, Manso AM, Okada H, Ross RS. Integrins and Integrin-Associated Proteins in The Cardiac Myocyte. Circ. Research. 2014;114(3): 572–86.

Iyer RP, Jung M & Lindsey ML. Mmp-9 Signaling in The Left Ventricle Following Myocardial Infarction. A. J. of Phys. Heart and Circ. Phys. 2016;311(1): H190–H198.

Kawamura N, Kubota T, Kawano S, Monden Y, et al. Blockade of NF-Kb improves Cardiac Function and Survival without Affecting Inflammation in TNF-A-Induced Cardiomyopathy. 2005;66(3): 520–9.

Kawano S, Kubota T, Monden Y, Tsutsumi T, et al. Blockade of Nf-Kb improves Cardiac Function and Survival after Myocardial Infarction. 2006;291(3): H1337–44.

Khachigian LM. Early Growth Response-1 in Cardiovascular Pathobiology. Circulation Research. 2006;98(2): 186–91.

Kumar S, Wang G, et al. HIMF (Hypoxia Induced Mitogenic Factor)-Il (Interleukin)-6 Signaling Mediates Cardiomyocyte-Fibroblast Crosstalk to Promote Cardiac Hypertrophy and Fibrosis. Hypertension (Dallas, Tex.: 1979). 2019; 73:1058–70.

Lapointe MC, Mendez M, Leung A, Tao Z, Yang XP. Inhibition of Cyclooxygenase-2 Improves Cardiac Function After Myocardial Infarction in The Mouse. Am. J. Physiol. Heart Circ. Physiol. 2004;286: H1416–H1424.

Li R & Frangogiannis NG. Chemokines In Cardiac Fibrosis. Current Opinion in Physiology. 2021;19: 80–91.

Liu HY, Yu LF, Zhou TG, Wang YD, et al. Lipopolysaccharide-Stimulated Bone Marrow Mesenchymal Stem Cells-Derived Exosomes Inhibit H2O2-Induced Cardiomyocyte Inflammation and Oxidative Stress Via Regulating mir-181a-5p/Atf2 Axis. European Review for Medical & Pharmacological Sciences. 2020;24(19).

Liu X, Zhang Y, Du W, Liang H, He H, Zhang L, et al. Mir-223-3p As a Novel MicroRNA Regulator of Expression of Voltage-

Gated K+ Channel Kv4.2 In Acute Myocardial Infarction. Cell Physiol Biochem. 2016;39: 102–14.

Marques FZ, Vizi D, Khammy O, et al. The Transcardiac Gradient of Cardio-MicroRNAs in the Failing Heart. Euro. Journal of Heart Failure. 2016;18(8): 1000–8.

Meléndez GC, Mclarty JL, Levick SP, Du Y, Janicki JS, Brower GL. Interleukin-6 Mediates Myocardial Fibrosis, Concentric Hypertrophy and Diastolic Dysfunction in Rats. Hypertension. 2010;56(2): 225–31.

Murtha LA, Schuliga MJ, Mabotuwana NS, Hardy SA, Waters DW, Burgess JK, Knight DA, & Boyle AJ. The Processes and Mechanisms of Cardiac and Pulmonary Fibrosis. Frontiers in Physiology. 2017;8, 777.

Ogata H, Goto S, Sato K, Fujibuchi W, Bono H, Kanehisa M. KEGG: Kyoto Encyclopedia of Genes and Genomes. Nucleic Acids Research. 1999;27(1): 29–34.

Qin D, Wang X, Li Y, Yang L, et al. MicroRNA 223-5p and−3p Cooperatively Suppress Necroptosis in Ischemic/Reperfused Hearts. J Biol Chem. 2016;291: 20247–59.

Rayner BS, et al. Selective Inhibition of the Master Regulator Transcription Factor Egr1 with Catalytic Oligonucleotides Reduces Myocardial Injury and Improves Left Ventricular Systolic Function in A Preclinical Model of Myocardial Infarction. 2013;2(4).

Reid BG, et al. Discovery of Novel Small Molecule Inhibitors of Cardiac Hypertrophy using High Throughput, High Content Imaging. J Mol Cell Card. 2016;97: 106–113.

Ren R, Ma K, Jiang Y, Chen J, Kou Y, Ge Z, et al. Endothelial Mir-196b-5p Regulates Angiogenesis via the Hypoxia/Mir-196b-5p/Hmga2/Hif1α Loop. American Journal of Physiology-Cell Physiology. 2023;324(2): C407–19.

Rollins BJ. Monocyte Chemoattractant Protein 1: A Potential Regulator of Monocyte Recruitment in Inflammatory Disease. Mol. Medicine Today. 1996;2(5): 198–204.

Rumzhum NN & Ammit AJ. Cyclooxygenase 2: Its Regulation, Role and Impact in Airway Inflammation. Clin. Exp. Allergy. 2016;46 (3): 397–410.

Saadat S, Noureddini M, et al. Pivotal Role of TGF-B/Smad Signaling in Cardiac Fibrosis: Noncoding RNAs as Effectual Players. Frontiers in Cardio. Medicine. 2021;7.

Samanta S, Balasubramanian S, Rajasingh S, Patel U, Dhanasekaran A, Dawn B, Rajasingh J. MicroRNA: A new therapeutic strategy for cardiovascular diseases. Trends in Cardiovascular Medicine. 2016;26(5), 407-419.

Santos DG, Resende MF, Mill JG, et al. Nuclear Factor (NF)-Kb Polymorphism is Associated with Heart Function in Patients with Heart Failure. BMC Med. Gen. 2010;11(1).

Schafer S, Viswanathan S, Widjaja AA, et al. IL-11 is A Crucial Determinant of Cardiovascular Fibrosis. Nature. 2017;552 (7683): 110–115.

Seidenberg J, Stellato M, Hukara A, Ludewig B, et al. The Ap-1 Transcription Factor Fosl2 Regulates Autophagy in Cardiac Fibroblasts During Myocardial Fibrogenesis. International Journal of Molecular Sciences. 2021;22(4): 1861.

Shannon P, Markiel A, et al. Cytoscape: A Software Environment for Integrated Models of Biomolecular Interaction Networks. Genome Res. 2003;13(11): 2498–504.

Sisto M, Lisi S. Targeting Interleukin-17 As A Novel Treatment Option for Fibrotic Diseases. J. Clin. Med. 2024;13, 164.

Smeets PJ, Teunissen, BE, et al. Cardiac hypertrophy is enhanced in PPARα−/− mice in response to chronic pressure overload. Cardio Research. 2008;78(1), 79-89.

Song J, et al. Microrna-122-5p Aggravates Angiotensin II-Mediated Myocardial Fibrosis and Dysfunction in Hypertensive Rats by Regulating the Elabela/Apelin-Apj and Ace2-Gdf15-Porimin Signaling. J. Of Cardio. Trans. Res. 2022;15: 535–547.

Stellato M, Dewenter M, Rudnik M, Hukara A, Özsoy Ç, Renoux F, et al. The Ap-1 Transcription Factor Fosl-2 Drives Cardiac Fibrosis and Arrhythmias Under Immunofibrotic Conditions. Communications Biology. 2023;6(1): 161.

Sun X, Sit A, Feinberg MW. Role Of Mir-181 Family in Regulating Vascular Inflammation and Immunity. Trends Cardiovasc Med. 2014;24: 105–112.

Szklarczyk D, Gable AL, et al. String V11: Protein–Protein Association Networks with Increased Coverage, Supporting Functional Discovery in Genome-Wide Experimental Datasets. Nucleic Acids Research. 2019;47(Database Issue): D607–13.

Tang Q, Li My, Su YF, Fu J, Zou ZY, Wang Y, et al. Absence of Mir-223-3p Ameliorates Hypoxia-Induced Injury by Repressing Cardiomyocyte Apoptosis and Oxidative Stress by Targeting Klf15. Eur J Pharmacol. 2018;841: 67–74.

Tarnavski O, Mcmullen Jr, Schinke M, Nie Q, et al. Mouse Cardiac Surgery: Comprehensive Techniques for Generating Mouse Models of Human Diseases and Their Application for Genomic Studies. Physio. Genomics. 2004;16(3): 349–60.

Tas SW, et al. Gene Therapy Targeting Nuclear Factor-Kappa B: Towards Clinical Application in Inflammatory Diseases and Cancer. Am Heart J. 2009; 9:160–70.

Travers JG, Tharp CA, Rubino M, Mckinsey TA. Therapeutic Targets for Cardiac Fibrosis: from Old School to Next-Gen. J. of Clinical Investigation. 2022;132(5).

Vidal S, Puig L, Carrascosa-Carrillo JM, González-Cantero Á, Ruiz-Carrascosa JC, Velasco-Pastor AM. From messengers to receptors in psoriasis: the role of IL-17RA in disease and treatment. International journal of molecular sciences. 2021; 22(13), 6740.

Wang L, Feng J, Deng Y, Yang Q, Wei Q, et al. CCAAT/Enhancer-Binding Proteins in Fibrosis: Complex Roles Beyond Conventional Understanding. Research. 2022a

Wang F, Zhang J, Niu G, Weng J, et al. Apigenin Inhibits Mice's Isoproterenol-induced Myocardial Fibrosis and SMAD Pathway by Regulating Oxidative Stress and mir-122-5p/155-5p Expressions. Drug Development Res. 2022b;83(4): 1003–15.

Wang J, Liew OW, Richards AM, Chen YT. Overview of MicroRNAs in Cardiac Hypertrophy, Fibrosis, and Apoptosis. Int'l J. of Mol. Sciences. 2016;17(5):749.

Wang M, Zhang W, Zhu J, Fu G, Zhou B. Breviscapine Ameliorates Hypertrophy of Cardiomyocytes Induced by High

Glucose in Diabetic Rats via the PKC Signaling Pathway. Acta Pharmacologica Sinica. 2009;30(8): 1081–91.

Wang Y, Jiao L, Qiang C, et. al. The Role of Matrix Metalloproteinase 9 in Fibrosis Diseases and its Molecular Mechanisms. Bio & Pharma. 2024;171, 116116.

Weng CH, Chung FP, Chen YC. et al. Pleiotropic Effects of Myocardial Mmp-9 Inhibition to Prevent Ventricular Arrhythmia. Sci Rep. 2016;6, 38894.

Whitehead AJ, Atcha H, Hocker JD, et al. AP-1 signaling modulates cardiac fibroblast stress responses. Journal of Cell Science. 2023;136(23), jcs261152.

Yang M, Huang Z-A, Gu W, Han K, Pan W, Yang X, Zhu Z. Prediction of biomarker–disease associations based on graph attention network and text representation. Briefings in Bioinformatics. 2022;23(5).

Yuan Y, Lin D, Feng L, Huang M, Yan H, Li Y, et al. Upregulation of mir-196b-5p Attenuates BCG Uptake Via Targeting SOCS3 and activating STAT3 in Macrophages from Patients with Long-Term Cigarette Smoking-Related Active Pulmonary Tuberculosis. Journal of Translational Medicine. 2018;16: 1–3.

Yun W, Qian L, Yuan R., Xu H. Periplocymarin Protects Against Myocardial Fibrosis Induced by B-Adrenergic Activation in Mice. Biomed. & Phar. 2021;139, 111562.

Zhang N, Wei WY, Li LL, et al. Therapeutic Potential of Polyphenols in Cardiac Fibrosis. Front Pharmacol. 2018;9: 122.

Zhang YL, Bai J, Yu WJ, Lin QY, Li HJ. Cd11b Mediates Hypertensive Cardiac Remodeling by Regulating Macrophage Infiltration and Polarization. Journal of Advanced Research. 2024;55, 17–31.

Zhou Y, Zhou B, Pache L, Chang M, Khodabakhshi AH, Tanaseichuk O, et al. Metascape Provides a Biologist-Oriented Resource for the Analysis of Systems-Level Datasets. Nature Communications. 2019;10(1): 1523.

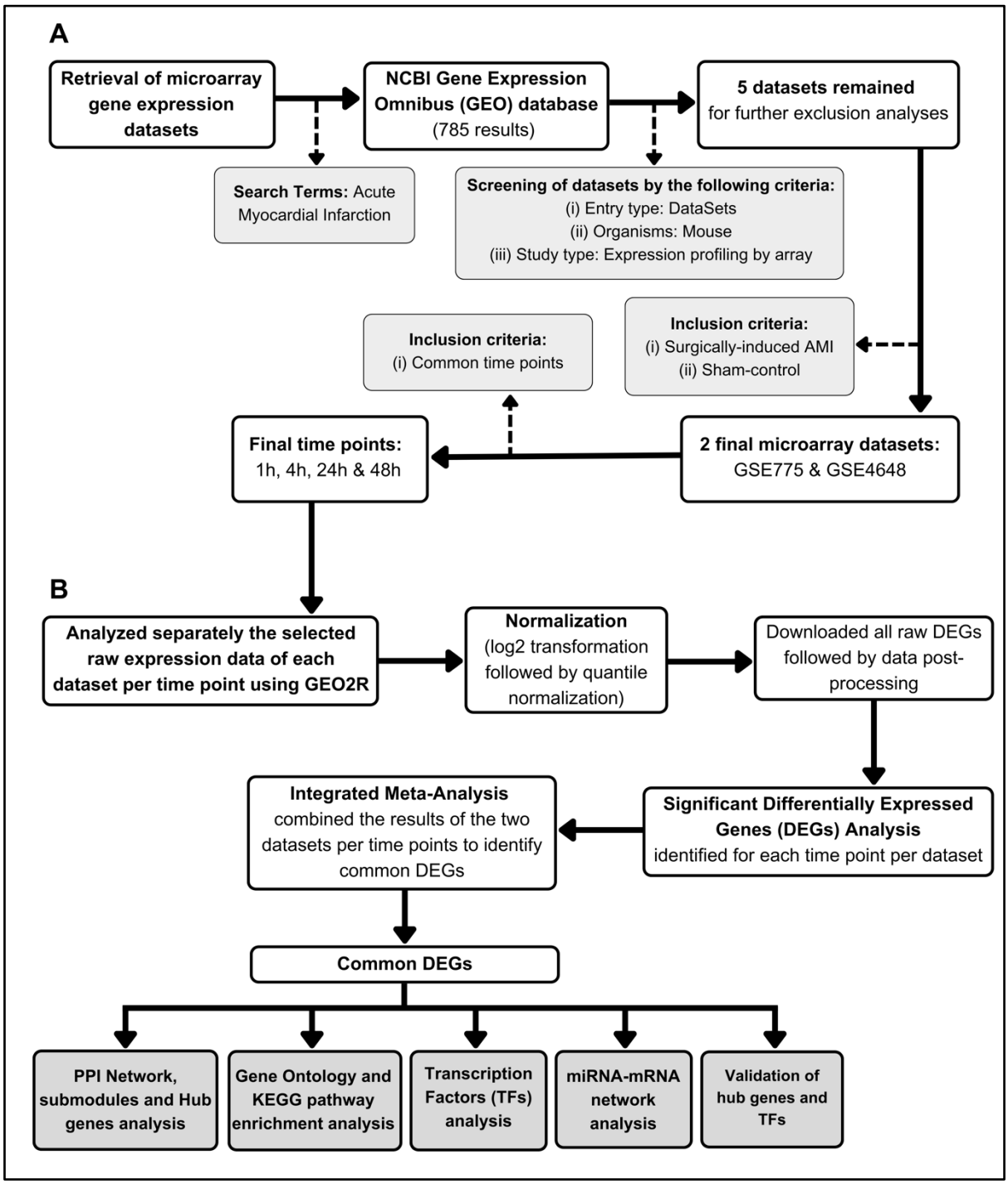


**Supplemental Figure 1: Workflow of microarray integrated meta-analysis.** (**A**) The selection process of eligible microarray datasets for the shared signatures between AMI and the mouse model. (**B**) Depiction of the flow chart of the process involved in the integrated meta-analysis of the selected microarray datasets.

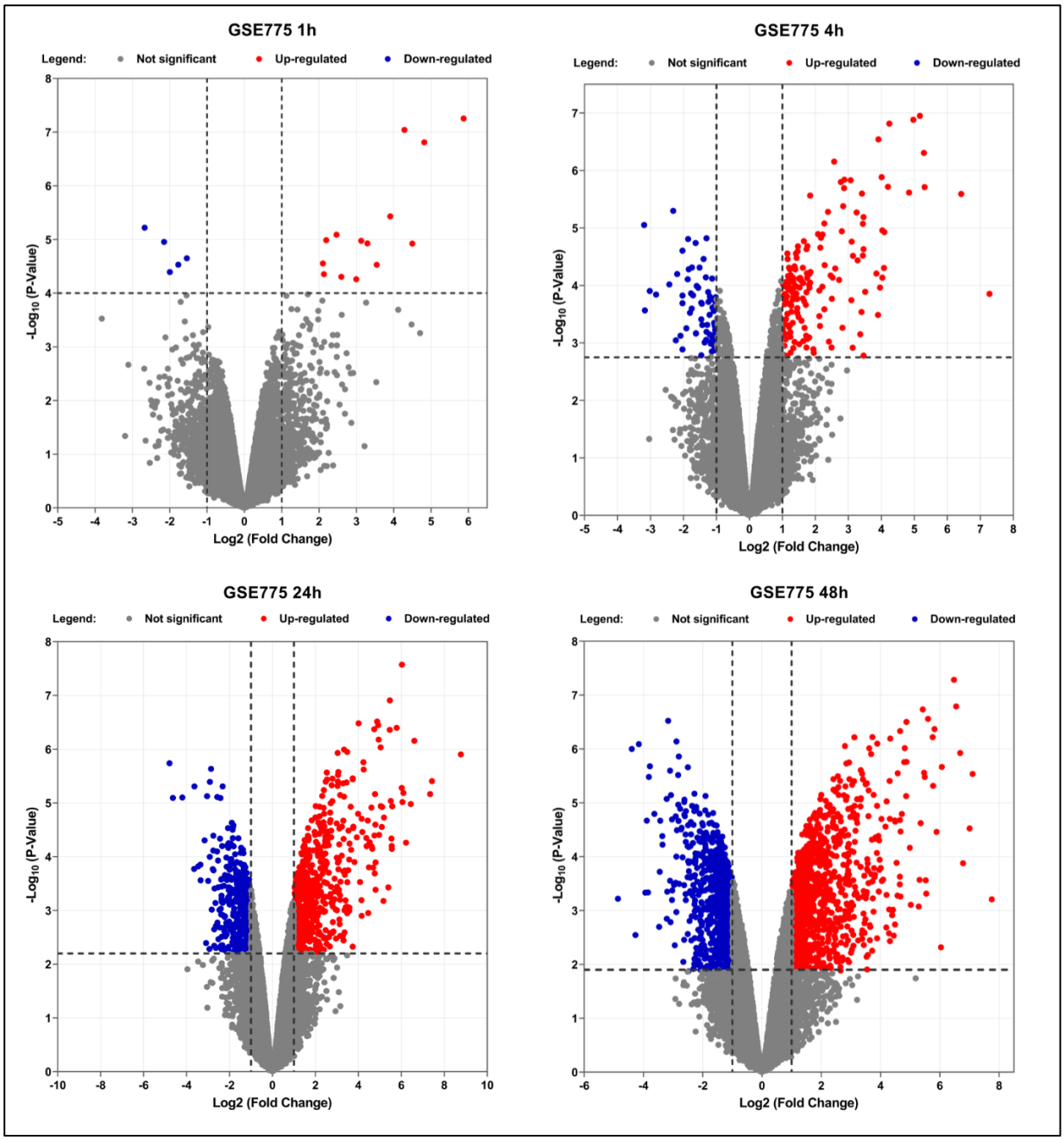


**Supplemental Figure 2: Volcano plot displaying the DEGs of GSE775 at different time points.** Blue points represent downregulated genes, red points represent upregulated genes, and gray points represent genes showing no significant difference in expression between AMI and control (the threshold for significance: |log2FC| > 1.0 at adjusted p-value < 0.05). The P value was adjusted using the Benjamini–Hochberg (false discovery rate) procedure.

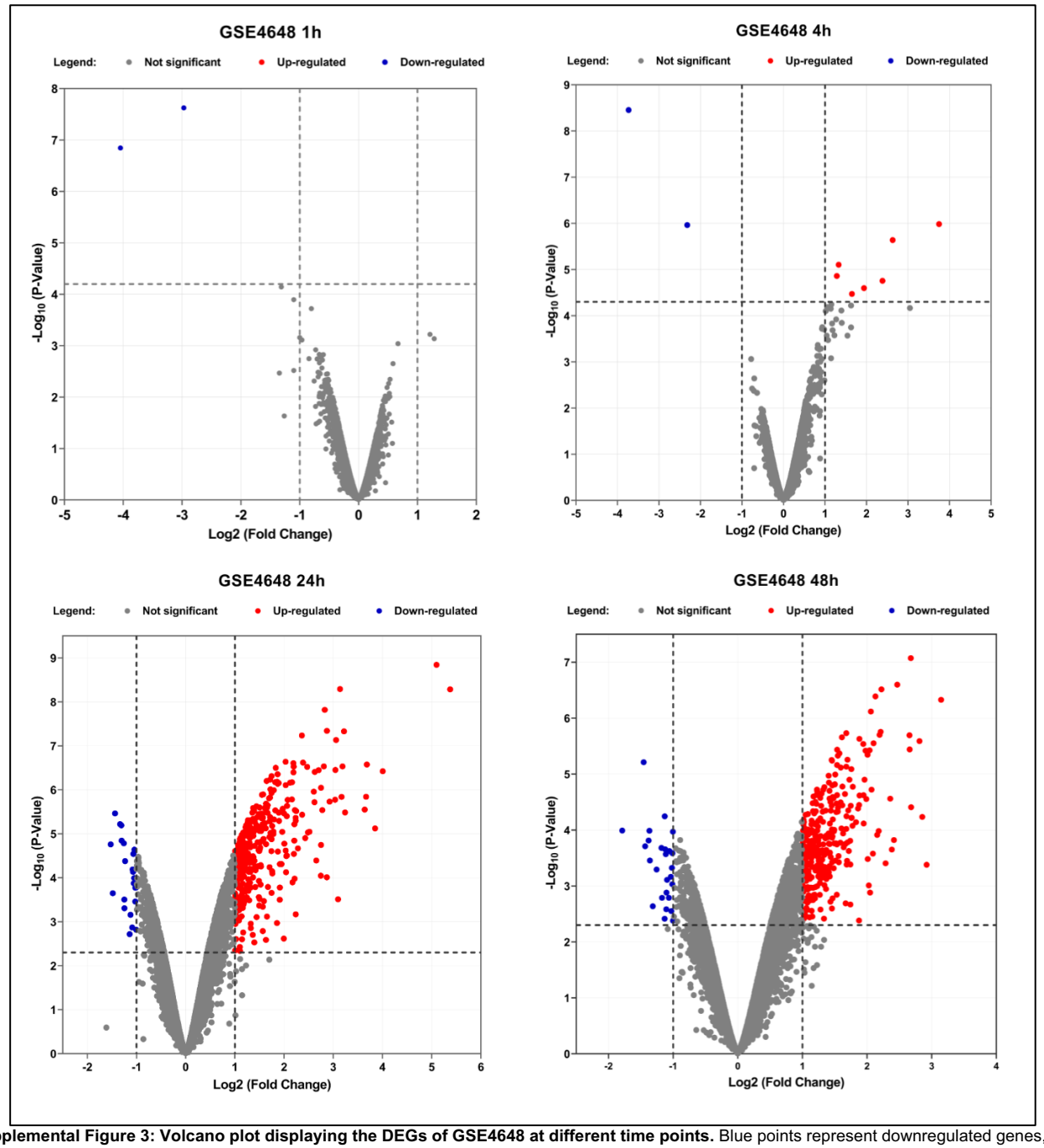


**Supplemental Figure 3: Volcano plot displaying the DEGs of GSE4648 at different time points.** Blue points represent downregulated genes, red points represent upregulated genes, and gray points represent genes showing no significant difference in expression between AMI and control (the threshold for significance: |log2FC| > 1.0 at adjusted p-value < 0.05). The P value was adjusted using the Benjamini–Hochberg (false discovery rate) procedure.

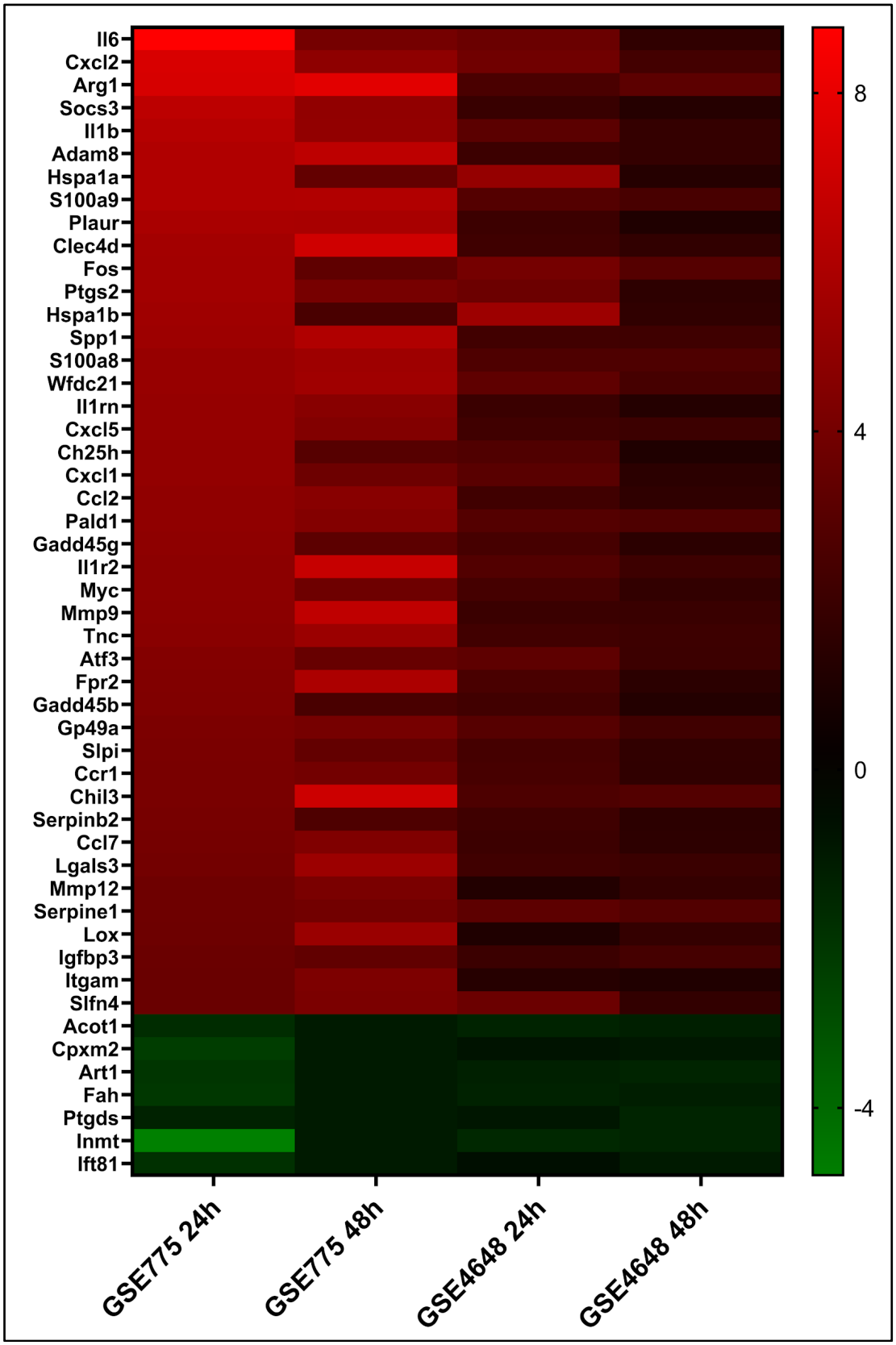


**Supplemental Figure 4: Heatmap of the common DEGs expressed in both GSE775 and GSE4648 at 24 h and 48 h.** Each column represents the dataset at a specific time point, and each row indicates the DEGs showing common upregulated DEGs (red) and downregulated DEGs (green). The color shading indicates the magnitude of differential expression (|$Log_2FC$| value).

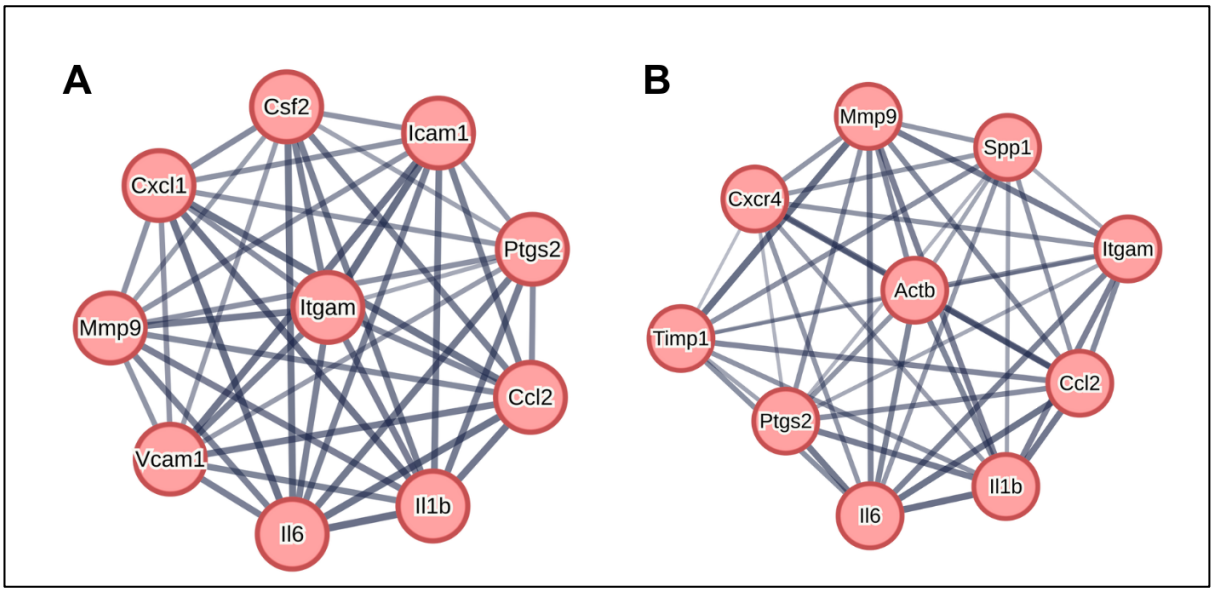


**Supplemental Figure 5: Hub genes identified using the MCC plug-in of cytoHubba.** Network of all identified Hub genes for the combined data at (**A**) 24h and (**B**) 48h.

**Supplemental Table 1: Differentially expressed genes (DEGs) between AMI group sham-control group.** |Log2FC| > 1 and an adjusted p-value of < 0.05

| **A. Differentially expressed genes per dataset per time points** | | | | | |
|---|---|---|---|---|---|
| **Datasets** | **Expression Level** | **1 h** | **4 h** | **24 h** | **48 h** |
| GSE775 | Upregulated | 14 | 159 | 597 | 1,075 |
| | Downregulated | 5 | 72 | 503 | 939 |
| | **Total DEGs** | **19** | **231** | **1,100** | **2,014** |
| | **Grand Total DEGs** | **3,364** | | | |
| GSE4648 | Upregulated | 0 | 7 | 353 | 346 |
| | Downregulated | 2 | 2 | 23 | 26 |
| | **Total DEGs** | **2** | **9** | **376** | **372** |
| | **Grand Total DEGs** | **759** | | | |
| **B. Common upregulated and downregulated DEGs per time points between GSE775 & GSE4648** | | | | | |
| | **Expression Level** | **1 h** | **4 h** | **24 h** | **48 h** |
| | Upregulated | 0 | 6 | 250 | 280 |
| | Downregulated | 0 | 0 | 13 | 22 |
| | **Total DEGs** | **0** | **6** | **263** | **302** |
| | **Grand Total DEGs** | **571** | | | |

**Supplemental Table 2: Common upregulated and downregulated DEGs at different time points.** |Log2FC| > 1 and an adjusted p-value of < 0.05

| Time point | Upregulated | Downregulated |
|---|---|---|
| 1h | none | none |
| 4h | Bhlhe40 Egr1 Hspa1b Gadd45g Fos Atf3 | none |
| 24h | Dnajb1 Mapk6 Ccl6 Angptl4 Bhlhe40 Tgif1 Fam107b Nop16 Mmp8 Capza1 Dusp6 Angpt2 Cd24a Tyrobp Slc11a1 Nip7 Gadd45b Txnrd1 Ndrg1 Atf4 Acsl4 Odc1 Capg Synpo Inhbb Napsa Ier2 Tubb6 Slpi Il17ra Fosl1 Ltb Rhoc Ccl7 Ereg Chil3 Il4ra Gm12854 /// Gm5068 /// LOC102637129 /// S100a11 Ccl12 Plac8 | Selenbp1 Cpxm2 Cdkn1c Inmt Fah Mettl20 Ift81 Art1 Acot1 Ptgds Gmnn Ttc30b Ank1 |

| | | |
|---|---|---|
| | 2610042L04Rik /// Gm10340 /// Gm10406 /// Gm10409 /// Gm16525 /// Gm2897 /// Gm3002 /// Gm3095 /// Gm3115 /// Gm3164 /// Gm3173 /// Gm3239 /// Gm3252 /// Gm3264 /// Gm3373 /// Gm3383 /// Gm3500 /// Gm3558 /// Gm3636 /// Gm3642 /// Gm3667 /// Gm3696 /// Gm3739 /// Gm5796 /// Gm6356 /// LOC100861615 /// LOC102638110 Kit Tpm4 Gsr Rassf5 Rtn4 Ppan Fhl1 Hbegf Vcan Gm9835 /// Gmfg Bcl2a1a /// Bcl2a1c /// Bcl2a1d Fcgr2b Timp1 Slc20a1 Cd52 Myc Pglyrp1 Dab2 Fam49b Fpr1 Uck2 Socs3 Tfpi2 Litaf Map3k8 Klf6 Cd14 Arg2 Tiparp Gna13 Sele Csf3r Cxcl2 F10 Gdf15 Ccl2 Gm11787 /// Lyn Lox Cmip Upp1 Marcksl1 S100a8 Vcam1 Plaur Cldn5 Itga5 Ncf2 Csf2 Adam8 Ptgs2 Cytip Ctgf Rasd1 Icam1 Thbd Kdelr3 Ccr2 Gm10693 /// Gm14548 /// Gm15448 /// Lilra6 /// Pira1 /// Pira11 /// Pira2 /// Pira4 /// Pira5 /// Pira6 /// Pira7 /// Pirb S100a9 Fos Myh9 Gch1 Cxcl5 Eno1 /// Eno1b Nop56 Atf3 Wfdc21 Errfi1 Pald1 /// Thbs1 Itgam Tgfbi Procr Nfe2 2610042L04Rik /// Gm10340 /// Gm10409 /// Gm16525 /// Gm2897 /// Gm3002 /// Gm3095 /// Gm3115 /// Gm3164 /// Gm3173 /// Gm3239 /// Gm3264 /// Gm3373 /// Gm3383 /// Gm3500 /// Gm3558 /// Gm3636 /// Gm3642 /// Gm3667 /// Gm3696 /// Gm3739 /// Gm5796 /// Gm6337 /// Gm6356 /// LOC100861615 /// LOC102638110 Fubp1 Sertad1 Iqgap1 Cxcr2 Hck Ero1l Slfn4 Cd44 Nppb Ctss Ugdh Ctsz LOC102633627 /// LOC102641281 /// Tpm4 Ankrd2 Diap1 Casp4 Tmem45a Pprc1 Tpd52 Il1r2 Egr1 Pvr Selplg Bcl2a1a /// Bcl2a1b /// Bcl2a1c /// Bcl2a1d /// Mthfs Ccl9 Adss Xirp1 Phlda1 Selp Actg1 Cyr61 Ch25h Msn Wsb1 Gadd45g Ier3 Aldh1a2 Sphk1 Emp1 Zfp36 Gp49a /// Lilrb4 Junb Pgm1 Clec4d Cd53 Ncf4 Nppa Pdlim7 Igfbp3 Sat1 Glrx Hmox1 Spp1 Basp1 Sdcbp Slfn3 /// Slfn4 Btg1 Rnf149 Mest Utp18 Ngf Adm Akap12 Nes Gp49a Itgb2 Anxa2 Slc2a1 Hp Nop58 Hif1a Nfil3 Fxyd5 Serpine1 Fpr2 Plk2 Il1rn Syncrip Gnl3 Ccr1 Fgl2 Pdpn Slc39a6 Mmp12 Azin1 Irg1 Lcp2 Mmp9 Rell1 Ptpn1 Il6 Ell2 Smad1 Hdc Il1b Hsp90aa1 Hspa1b Eif1a Slfn1 Serpinb2 Clic1 /// Sept9 Lgals3 Nifk Rassf1 Pfkp Lrrfip1 Snhg1 Enah Tnc Tes Msr1 Srgn Apbb1ip Ctla2b Id2 Ptpn2 Irf8 Sema7a Ctla2a /// Ctla2b Ptx3 Psat1 Rasl11b Lcp1 Ifitm6 Nfkbiz Ifrd1 Hspa1a Cxcl1 Actn1 Fndc3a Slfn2 Osmr Ptpre Vasp Arg1 | |
| 48h | BC037034 Mcam Pabpc1 Tram1 Mmp8 Actn4 Ifi30 Mcm3 Cd24a Tyrobp Gadd45b Ndrg1 Acsl4 Cmtm3 Odc1 Synpo Tagln2 Nme1 Tubb6 Tmsb10 Cfl1 Ccl7 Gm12854 /// Gm5068 /// LOC102637129 /// S100a11 Plac8 Atxn10 Dynll1 Rtn4 Fhl1 Hbegf Nid2 Ppp1r14b Timp1 Slc20a1 Cd52 Rgs19 Myc Prmt1 Fam49b Fpr1 Lrrc59 D17H6S56E-5 Litaf Srsf9 Pla2g7 Cxcl2 Flnb Plaur Uba5 Nras Ncf2 Ptgs2 Cytip Npm1 Ctgf Creld2 Ccr2 Gm10693 /// Gm14548 /// Gm15448 /// Lilra6 /// Pira1 /// Pira11 /// Pira2 /// Pira4 /// Pira5 /// Pira6 /// Pira7 /// Pirb Fos S100a9 Crct1 Eno1 /// Eno1b Nop56 Atf3 Wfdc21 Procr Edem1 Nppb Ctss Ctsz LOC102633627 /// LOC102641281 /// Tpm4 Ankrd2 S100a10 Il1r2 Wbp5 Selplg Akr1b8 Ccl9 Cyr61 Wsb1 Nsun2 Gadd45g Anp32b Clec4d Col18a1 Ncf4 Lyz1 /// Lyz2 Igfbp3 Cks2 Spp1 Basp1 Rnf149 Btg1 Mest Ngf Evi2a Itgb2 Anxa2 Serpine1 Fpr2 Il1rn Pdpn Azin1 Mmp9 Rell1 Prkcdbp Il6 Ell2 Eif1a Ctsc Clic1 /// Sept9 Casp3 Nifk Lgals3 Rassf1 Pfkp Lrrfip1 Rcan1 Msr1 Srgn Apbb1ip Ctla2b Ampd3 Ctla2a /// Ctla2b Rasl11b Lcp1 Ptprc Nhp2 Map2k1 Eps8 Hspa1a Col4a1 Acsl5 Actn1 Fndc3a Tubb2a Osmr Arg1 Mapk6 Cnn2 Tuba1a Pdk3 Cct3 Tardbp Tgif1 Nop16 Pcna Ptbp3 Capza1 Angpt2 Stbd1 Txnrd1 Tmem167 Postn Capg Usp1 Cxcr4 Mmp3 Slpi Anxa1 Mfap5 Tsr1 Morf4l2 Acot9 Chil3 Tpm4 Gsr Cks1b Bcl2a1a /// Bcl2a1c /// Bcl2a1d Fcgr2b Sgpl1 Pglyrp1 Uck2 Socs3 Col5a2 Mob1a Tfpi2 Tubb5 Cd14 Gna13 Manf F10 Ccl2 Lox Sfxn1 Marcksl1 S100a8 Fcgr1 Ccr5 Itga5 Adam8 Arhgap1 Rbp1 Sfpq Kdelr3 Myh9 Cxcl5 Errfi1 Pald1 /// Thbs1 Tgfbi Itgam Fam13b Sprr1a Iqgap1 Hck Ero1l Spi1 Slfn4 Snrpa1 Ugdh Diap1 Adam9 Tmem45a Tpd52 Bcl2a1a /// Bcl2a1b /// Bcl2a1c /// Bcl2a1d /// Mthfs Adss Ch25h Msn D15Ertd621e Ier3 Gp49a /// Lilrb4 Cyba Pgm1 Arf6 Cd53 Nppa Pgam1 Pdlim7 Pdia6 Rbms1 Nucb2 Nes Gp49a Gusb Cdr2 Slc2a1 Hp Fbln2 Nop58 Fxyd5 Smc2 Lxn Ccr1 Slc39a6 Rrbp1 Mmp12 Cfp Crlf1 Coro1c Ptpn1 Sec61a1 Smad1 Il1b Hsp90aa1 Hspa1b Cd68 Slfn1 Serpinb2 S100a4 Atp13a3 Vcl Csrp1 Tnc Enah Tes Lmna Sema7a Psat1 Bgn Fkbp1a Srm Ifitm6 Nfkbiz Cyfip1 Anxa3 Cotl1 Ifrd1 Tuba1c Cxcl1 Vasp Cd93 | Tcea3 Hsdl2 Hadh Sult1a1 Slc2a4 Pla2g12a Aqp1 Sesn1 Mgst3 Cpxm2 Adh1 Inmt Fah Mlf1 Thrsp Echs1 Ift81 Art1 Acot1 Ptgds Eci1 Pxmp2 |

**Supplemental Table 3:** Key transcription factors (TFs) of hub genes.

| Key TF | Description | Hub genes | *p-value* |
|---|---|---|---|
| NFKB1 | *nuclear factor of kappa light polypeptide gene enhancer in B cells 1, p105* | *IL1b, Itgam, Ccl2, Mmp9, IL6, Ptgs2* | *8.36E-13* |
| Jun | jun proto-oncogene | IL1b, Ccl2, Mmp9, IL6, Ptgs2 | 6.11E-11 |
| Rela | v-rel reticuloendotheliosis viral oncogene homolog A (avian) | Ccl2, Mmp9, IL6, Ptgs2 | 1.77E-08 |
| *Cebpb* | *CCAAT/enhancer binding protein (C/EBP), beta* | *IL1b, IL6, Ptgs2* | *1.63E-07* |
| Sp1 | trans-acting transcription factor 1 | Ccl2, Mmp9, IL6, Ptgs2 | 4.46E-07 |
| Ets1 | E26 avian leukemia oncogene 1, 5' domain | Ccl2, Mmp9, Ptgs2 | 4.60E-07 |
| Ep300 | E1A binding protein p300 | Mmp9, IL6, Ptgs2 | 4.85E-07 |
| *Egr1* | *early growth response 1* | *IL1b, Ccl2, Mmp9* | *8.08E-07* |
| Etv4 | ets variant 4 | Mmp9, Ptgs2 | 7.60E-06 |
| Ahr | aryl-hydrocarbon receptor | IL6, Ptgs2 | 1.67E-05 |
| Sirt1 | sirtuin 1 | Mmp9, IL6 | 2.35E-05 |
| Rel | reticuloendotheliosis oncogene | IL1b, Ccl2 | 2.73E-05 |
| *Ppara* | *peroxisome proliferator activated receptor alpha* | *IL6, Ptgs2* | *7.46E-05* |
| Smad3 | SMAD family member 3 | Ccl2, Mmp9 | 8.47E-05 |
| *Fos* | *FBJ osteosarcoma oncogene* | *Mmp9, IL6* | *0.000111* |
| Stat3 | signal transducer and activator of transcription 3 | Mmp9, IL6 | 0.000221 |
| Sp3 | trans-acting transcription factor 3 | IL6, Ptgs2 | 0.000244 |